Derivation, Modelling and Solution of the Conditionally Averaged Two-Phase Flow Equations

H.G. Weller
Department of Mechanical Engineering
Imperial College of Science Technology and Medicine

15th July 1999

Abstract

This report outlines the development of a general purpose, robust and stable numerical algorithm for the solution of industrial two-phase flow problems. Particular attention is paid the the issues of phase-inversion and complete phase separation; these being two of the most difficult problems to handle numerically. The derivation, using conditional averaging, of the two-phase equations is outlined followed by the manipulation necessary to cast the equations in a form suitable for numerical solution. The discretised form of the equations is presented in the code independent finite-volume notation of Weller [1] followed by the solution algorithm. Two-phase modelling, in particular turbulence closure, is not covered in detail except where it influences the numerical algorithm. The models used here are those used in the BRITE II project, altered where necessary to obey a stricter set of physical constraints. No attempt has been made to demonstrate the accuracy of these developments; this is the subject for the BRITE III project.

Nomenclature

Normal symbols represent scalar quantities and boldface symbols represent vector and tensor quantities. Generally boldface roman symbols represent vector and bolface Greek symbols represent tensor quantities, but this rule is not adhered to religously. Dimensions and units are given in terms of the full SI set, *i.e.* mass (M) in kg, length (L) in meters (m), time (t) in seconds (s), temperature (T) in Kelvin (K), moles (m) in moles (mol), current (c) in Amperes (A) and luminous intensity (I) in candela (cd).

Roman Symbols

Symbol	Description	Dimensions	Units
A	Coefficient (*eg.* for drag model)	?	?
C	Dimensionless coefficient (*eg.* for drag model)	-	-
D	Diffusive transport term	$1/t$	$1/s$
$\mathcal{D}$	Diffusivity	L^2/t	m^2
$\mathbf{g}$	Acceleration due to gravity	L/t^2	m/s^2
I	Indicator function	-	-
$\mathbf{I}$	Identity matrix	-	-
k	Turbulence kinetic energy	L^2/t^2	J/kg
l	Turbulence integral length scale	L	m
$\mathbf{M}$	Interfacial momentum transfer rate	$M/(L^2t^2)$	$kg/(m^2s^2)$
$\mathbf{n}$	Unit normal	-	-
p	Pressure	M/Lt^2	Pa
$\mathbf{P}$	Tensor property of any rank	-	-
$\mathbf{Q}$	Tensor property of any rank	-	-
$\mathbf{R}$	Reynolds stress	L^2/t^2	m^2/s^2
S	Surface	L^2	m^2
S	Interface propagation speed	L/t	m/s
t	Time	t	s
$\mathbf{U}$	Velocity	L/t	m/s
$\mathbf{x}$	Spatial position	L	m

Greek Symbols

Symbol	Description	Dimensions	Units
α	Volume fraction	-	-
ε	Turbulence kinetic energy dissipation rate	L^2/t^3	J/kgs
μ	Dynamic viscosity	M/Lt	Ns/m^2
ν	Kinematic viscosity	M^2/t	m^2/s
ρ	Density	M/L^3	kg/m^3
Σ	Surface area per unit volume	1/L	1/n
σ	Stress tensor	M/Lt^2	Pa
τ	Deviatoric part of the stress tensor	M/Lt^2	Pa
Ξ	Total surface "wrinkling"	-	-

Subscripts

$\mathbf{Q}_a$	Value of $\mathbf{Q}$ in phase a
$\mathbf{Q}_b$	Value of $\mathbf{Q}$ in phase b
$\mathbf{Q}_c$	Value of $\mathbf{Q}$ in continuous phase
$\mathbf{Q}_d$	Value of $\mathbf{Q}$ in dispersed phase
$\mathbf{Q}_I$	Interface
$\mathbf{Q}_\varphi$	Value of $\mathbf{Q}$ in phase φ
$\mathbf{Q}_r$	Relative Value of $\mathbf{Q}$ between two phases
$\mathbf{Q}_s$	Surface
$\mathbf{Q}_t$	Turbulent

Superscripts

$\mathbf{Q}^T$	Transpose
$\mathbf{Q}'$	Integration parameter
$\mathbf{Q}'$	Fluctuation with respect to ensemble average
$\mathbf{Q}''$	Fluctuation with respect to density weighted ensemble average
$\mathbf{Q}^\sharp$	Fluctuation with respect to interface average

Oversymbols

$\overline{\mathbf{Q}}$	Ensemble average
$\overline{\mathbf{Q}}_\varphi$	Conditional ensemble average in phase φ
$\widetilde{\mathbf{Q}}$	Density weighted ensemble average in phase φ
$\widetilde{\mathbf{Q}}_\varphi$	Conditional density weighted ensemble average
$\widehat{\mathbf{Q}}$	Interface average
$\dot{\mathbf{Q}}$	Rate of change

1 Introduction

Following extensive testing of the two-phase algorithm developed during the BRITE II project, serious deficiencies became apparent. These manifest themselves as poor convergence behaviour, numerical instabilities and restrictions in range of operation. Initially it appeared that these problems might be remedied through minor adjustments of the algorithm and numerical schemes. The ease with which such alternatives may be implemented in FOAM allowed a very large number of strategies to be tested in a relatively short time. However, these trials did not support such an optimistic view of the BRITE II algorithm, rather it demonstrated the need for a significant redevelopment of the approach.

The ultimate aim of this work is to create a general and stable two-phase flow solution algorithm for complex industrial application. A frequent problem encountered is that of phase-inversion, for which it is not reasonable to assume either phase is continuous, but that either may dominate in different regions of the same flow; under extreme (but not uncommon) conditions either phase may not be present at all in some regions of the domain. This is a particularly difficult problem to handle numerically and requires special consideration. The failure of the BRITE II algorithm for industrial application appears in part to be a consequence of not considering these issues explicitly. Careful consideration of the phase-inversion problem has lead to an unusual set of numerical practices and algorithm elements which, when combined, form a robust, general and extensible approach to two-phase flow. This report describes all of the elements necessary to handle phase inversion but not complete separation as this creates very large density gradients which require special pressure interpolation practices on collocated grids. These practices are quite different from those currently used in STAR-CD and may involve significant implementation effort. However, if there is sufficient customer demand for the simulation of such extreme two-phase flow conditions then the alternative pressure algorithm currently used in FOAM could be implemented in STAR-CD. These details will be covered in a subsequent report.

The issues covered in this report are predominantly numerical, however, some of the analysis raises questions about the appropriateness of some of the models developed within the BRITE II project and by others; these points are covered in more detail. The issue of turbulence closure is avoided to a large extent as it does not impinge significantly on the major numerical problems, and is being handled by others as part of the BRITE III project. For completeness the derivation of the conditionally averaged multi-phase flow equations is first outlined. This is followed by the manipulation necessary to cast these equations in a form suitable for numerical solution. The algorithm is then described in sufficient detail for implementation in a general purpose CFD code. The advantages of the proposed approach over previous methods is outlined but also explaining possible limitations. The report concludes with proposals for further developments. A FOAM

code called bubbleFoam containing the algorithm described here will be made available to CD with a selection of pre-computed test cases. A separate report on this will be supplied.

2 Conditional Averaging

The techniques associated with conditional averaging are not as well known as those used in Reynolds averaging so before proceeding to conditionally average the equations for multi-phase flow a short summary of the techniques is presented. This work is a development of that previously published in [2] which is based on the work of Dopazo [3]. A more complete description of the application of conditional averaging to incompressible two-phase flow with particular emphasis on modelling and turbulence closure is presented in the PhD thesis of Hill [4].

Conditional averaging is applied to multi-phase flow by considering the phases to be separated by an infinitesimally thin interface. Equations are conditionally averaged by multiplying by an indicator function I_φ, which is 1 in phase φ and 0 in the other phases, and then applying a conventional averaging technique, density weighted or otherwise. This approach is a simple extension of that applied to intermittent turbulent flows by Dopazo [3], but using an indicator function rather than the intermittency function, and allowing the phase interface to propagate. In the present work conditional averaging will be applied by conditioning the equations with the indicator function and then applying density-weighted ensemble averaging for generality. This is appropriate for compressible flow with large phase density fluctuations but in the incompressible limit the equations revert to the standard non-density weighted forms and some simplification is possible. It is felt that the use of density weighted ensemble averaging does not add significantly to the complexity of the derivation and may prove useful in the future when this work is extended to compressible multi-phase flow.

The terms resulting from conditional averaging are manipulated and simplified by applying formulae presented in [3] and outlined below, replacing terms involving the indicator function with equivalent terms involving the phase volume fraction α_φ. A subscript φ is used to denote the conditional average of a property in that phase.

2.1 Formulae for Conditional Averaging

The indicator function $I_\varphi(\mathbf{x}, t)$ is defined as

$$I_\varphi(\mathbf{x}, t) = \begin{cases} 1 & \text{if point } (\mathbf{x}, t) \text{ is in phase } \varphi, \\ 0 & \text{otherwise.} \end{cases} \tag{1}$$

The phase volume fraction α_φ is calculated as the probability of point $(\mathbf{x}, t)$ being in phase φ *i.e.*

$$\alpha_\varphi = \overline{I_\varphi}(\mathbf{x}, t) \tag{2}$$

where the overbar denotes the ensemble average. It is also useful to define the phase mass fraction (which is equivalent to the density weighted volume fraction) $\widetilde{\alpha}_\varphi$ through the identity

$$\overline{\rho}\widetilde{\alpha}_\varphi \equiv \overline{\rho}_\varphi \alpha_\varphi. \tag{3}$$

Now let $\mathbf{Q}(\mathbf{x}, t)$ be any fluid property, scalar or tensor of any rank, then the conditional average of $\mathbf{Q}$, $\overline{\mathbf{Q}}_\varphi$ is defined by

$$\overline{I_\varphi \mathbf{Q}} = \alpha_\varphi \overline{\mathbf{Q}}_\varphi. \tag{4}$$

Similarly the density weighted conditional average of $\mathbf{Q}$, $\widetilde{\mathbf{Q}}_\varphi$, is defined by

$$\overline{I_\varphi \rho \mathbf{Q}} = \alpha_\varphi \overline{\rho}_\varphi \widetilde{\mathbf{Q}}_\varphi. \tag{5}$$

2.1.1 Conditional Fluctuations

The most convenient definition of conditional fluctuation is as the difference between the instantaneous and conditional average of the property, that is

$$\mathbf{Q}'_\varphi \equiv \mathbf{Q} - \overline{\mathbf{Q}}_\varphi. \tag{6}$$

This definition is chosen so that the conditional average of the conditional fluctuation is zero. Similarly, the density-weighted conditional fluctuation is defined as

$$\mathbf{Q}''_\varphi \equiv \mathbf{Q} - \widetilde{\mathbf{Q}}_\varphi, \tag{7}$$

but, as for the standard density weighted ensemble average, the average of this fluctuation is not zero unless it is density weighted.

2.1.2 Conditionally Averaging Products

Let $\mathbf{P}(\mathbf{x}, t)$ be another fluid property, scalar or tensor of any rank, then from Eqs. (4 and 6)

$$\overline{I_\varphi \mathbf{P}\mathbf{Q}} = \alpha_\varphi \overline{\mathbf{P}}_\varphi \overline{\mathbf{Q}}_\varphi + \alpha_\varphi \overline{\mathbf{P}'_\varphi \mathbf{Q}'_\varphi} \tag{8}$$

and from Eqs. (5 and 7)

$$\overline{I_\varphi \rho \mathbf{P}\mathbf{Q}} = \alpha_\varphi \overline{\rho}_\varphi \widetilde{\mathbf{P}}_\varphi \widetilde{\mathbf{Q}}_\varphi + \alpha_\varphi \overline{\rho}_\varphi \widetilde{\mathbf{P}''_\varphi \mathbf{Q}''_\varphi} \tag{9}$$

2.1.3 Conditionally Averaging Differential Operations

Since differentiation and ensemble averaging commute

$$\overline{\nabla I_\varphi \mathbf{Q}} = \nabla(\overline{I_\varphi \mathbf{Q}}) = \nabla(\alpha_\varphi \overline{\mathbf{Q}}_\varphi) \tag{10}$$

and

$$\overline{\frac{\partial I_\varphi \mathbf{Q}}{\partial t}} = \frac{\partial(\overline{I_\varphi \mathbf{Q}})}{\partial t} = \frac{\partial(\alpha_\varphi \overline{\mathbf{Q}}_\varphi)}{\partial t}. \tag{11}$$

Now consider the mean of $I_\varphi \nabla \mathbf{Q} = \nabla(I_\varphi \mathbf{Q}) - (\nabla I_\varphi)\mathbf{Q}$ over the control volume δV. Note ∇I_φ is non-zero only at the interface, where it has the absolute value of the Dirac delta function and the direction of the unit normal $\mathbf{n}_\varphi$ to the interface, pointing into phase φ. Then

$$\overline{I_\varphi \nabla \mathbf{Q}} = \nabla(\overline{I_\varphi \mathbf{Q}}) - \lim_{\delta V \to 0} \overline{\frac{1}{\delta V} \int_{S(\mathbf{x},t)} \mathbf{n}_\varphi \mathbf{Q}(\mathbf{x}, t)\, dS} \tag{12}$$

where $S(\mathbf{x}, t) = 0$ is the equation for the interface. The interface average $\widehat{\mathbf{Q}}$ of a property $\mathbf{Q}$ is defined as the surface integral per unit volume divided by the surface area per unit volume Σ :

$$\widehat{\mathbf{Q}} \equiv \frac{\lim_{\delta V \to 0} \overline{\frac{1}{\delta V} \int_{S(\mathbf{x},t)} \mathbf{Q}(\mathbf{x}, t)\, dS}}{\Sigma} \tag{13}$$

where

$$\Sigma \equiv \lim_{\delta V \to 0} \overline{\frac{a}{\delta V} \int_{S(\mathbf{x},t)} dS}. \tag{14}$$

Eqn. (12) may now be re-written as

$$\overline{I_\varphi \nabla \mathbf{Q}} = \nabla(\alpha_\varphi \overline{\mathbf{Q}}_\varphi) - \widehat{\mathbf{n}_\varphi \mathbf{Q}}\Sigma. \tag{15}$$

Also

$$\overline{I_\varphi \nabla \cdot \mathbf{Q}} = \nabla \cdot (\alpha_\varphi \overline{\mathbf{Q}}_\varphi) - \widehat{\mathbf{n}_\varphi \cdot \mathbf{Q}}\Sigma \tag{16}$$

and

$$\overline{I_\varphi \frac{\partial \mathbf{Q}}{\partial t}} = \frac{\partial \alpha_\varphi \overline{\mathbf{Q}}_\varphi}{\partial t} + \widehat{\mathbf{Q}\mathbf{n}_\varphi \cdot \mathbf{U}_s}\Sigma \tag{17}$$

where $\mathbf{U}_s$ is the velocity of the interface.

Useful identities are obtained by considering the simple case of $Q = 1$, then from Eqn. (15)

$$\widehat{\mathbf{n}_\varphi}\Sigma = \nabla \alpha_\varphi \tag{18}$$

and from Eqn. (17)

$$\frac{\partial \alpha_\varphi}{\partial t} = -\widetilde{\mathbf{n}_\varphi \bullet \mathbf{U}_s}\Sigma \tag{19}$$

The second identity is of particular importance in conditional averaging, it being the evolution equation for the mean interface distribution, which will be referred to as the interface transport equation. Although it would appear that an independent equation for the interface may be obtained from Eqn. (19) for both phases on either side of the interface, it is apparent that the equations are equivalent. For the present purpose this is as far as the analysis of the interface equation need be taken although it might be a useful in conjunction with the surface area density equation [5] as a starting point for the development of a model for bubble size distribution *etc.* .

3 Turbulent Multi-Phase Flow Equations

In what follows, the conditional averaging techniques outlined above are applied to the basic transport equations representing turbulent multi-phase flow. Although the current interest is in two-phase flow, at this stage in the analysis the generality of multi-phase flow does not require greater complexity.

3.1 Conditionally Averaged Continuity Equation

In addition to the interface equation presented in Section 2.1.3, the conditionally averaged continuity equation is required in the derivation and simplification of other transport equation. The continuity equation

$$\frac{\partial \rho}{\partial t} + \nabla \bullet \rho \mathbf{U} = 0 \tag{20}$$

is conditionally averaged by multiplying by the indicator function I_φ, ensemble averaginging and simplifying using Eqs. (16 and 17), resulting in

$$\frac{\partial \alpha_\varphi \overline{\rho}_\varphi}{\partial t} + \widetilde{\rho \mathbf{n}_\varphi \bullet \mathbf{U}_s}\Sigma + \nabla \bullet (\alpha_\varphi \overline{\rho_\varphi \mathbf{U}_\varphi}) - \widetilde{\rho \mathbf{n}_\varphi \bullet \mathbf{U}}\Sigma = 0. \tag{21}$$

Eqn. (21) may be further simplified by combining the two surface average terms and applying density weighted averaging to the $\rho\mathbf{U}$ correlation leading to

$$\frac{\partial \alpha_\varphi \overline{\rho}_\varphi}{\partial t} + \nabla \bullet (\alpha_\varphi \overline{\rho}_\varphi \widetilde{\mathbf{U}}_\varphi) = \widetilde{\rho \mathbf{n}_\varphi \bullet (\mathbf{U} - \mathbf{U}_s)}\Sigma \tag{22}$$

The difference between the interface velocity $\mathbf{U}_s$ and the fluid velocity $\mathbf{U}$ at the interface is of course the interface propagation velocity which may be expressed

in terms of the interface propagation speed S_φ, due to phase mass transfer and the interface normal $\mathbf{n}_\varphi$ as $S_\varphi \mathbf{n}_\varphi$. Applying this simplification, the final form of the conditionally averaged continuity equation is

$$\frac{\partial \alpha_\varphi \overline{\rho}_\varphi}{\partial t} + \nabla\bullet(\alpha_\varphi \overline{\rho}_\varphi \widetilde{\mathbf{U}}_\varphi) = -\widehat{\rho_\varphi S_\varphi}\Sigma \tag{23}$$

3.2 Conditionally Averaged Momentum Equation

The momentum equation for a compressible fluid under the influence of gravity may be written

$$\frac{\partial \rho \mathbf{U}}{\partial t} + \nabla\bullet(\rho \mathbf{U}\mathbf{U}) = -\nabla\bullet\boldsymbol{\sigma} + \rho\mathbf{g}. \tag{24}$$

The total stress tensor $\boldsymbol{\sigma}$ is traditionally decomposed into an isotropic part $\mathbf{I}p$, where p is the static pressure, and a deviatoric part $\boldsymbol{\tau}$ such that $\boldsymbol{\sigma} = \mathbf{I}p + \boldsymbol{\tau}$, in which case the momentum equation becomes

$$\frac{\partial \rho \mathbf{U}}{\partial t} + \nabla\bullet(\rho \mathbf{U}\mathbf{U}) = -\nabla p - \nabla\bullet\boldsymbol{\tau} + \rho\mathbf{g}. \tag{25}$$

For a Newtonian fluid $\boldsymbol{\tau} = -2\mu\,\mathrm{dev}(\,\mathrm{symm}(\nabla\mathbf{U})) = -\mu(\nabla\mathbf{U} + \nabla\mathbf{U}^T - \frac{2}{3}\mathbf{I}\nabla\bullet\mathbf{U})$ although this assumption need not be made here as it does not affect the development of the solution algorithm and so the general form is maintained.

The conditionally averaged momentum equation is derived in a manner analogous to the continuity equation, multiplying Eqn. (25) by the indicator function I_φ, averaging, simplifying using Eqs. (17, 16, 15 and 8) and applying density weighting to the averages of correlations, Eqn. (9), resulting in

$$\begin{aligned}\frac{\partial \alpha_\varphi \overline{\rho}_\varphi \widetilde{\mathbf{U}}_\varphi}{\partial t} + \widehat{\rho\mathbf{U}\mathbf{n}_\varphi\bullet\mathbf{U}_s}\Sigma + \nabla\bullet(\alpha_\varphi \overline{\rho}_\varphi \widetilde{\mathbf{U}}_\varphi \widetilde{\mathbf{U}}_\varphi) + \nabla\bullet(\alpha_\varphi \overline{\rho}_\varphi \widetilde{\mathbf{U}''_\varphi \mathbf{U}''_\varphi}) - \widehat{\rho\mathbf{U}\mathbf{n}_\varphi\bullet\mathbf{U}}\Sigma \\ = -\nabla(\alpha_\varphi \overline{p}_\varphi) + \widehat{\mathbf{n}_\varphi p}\Sigma - \nabla\bullet(\alpha_\varphi \overline{\boldsymbol{\tau}}_\varphi) + \widehat{\mathbf{n}_\varphi\bullet\boldsymbol{\tau}}\Sigma - \alpha_\varphi \overline{\rho}_\varphi \mathbf{g}\end{aligned} \tag{26}$$

The l.h.s. of Eqn. (26) can be simplified by combining the two interface average terms, noting that $S_\varphi \mathbf{n}_\varphi = \mathbf{U}_s - \mathbf{U}$. The density weighted phase Reynolds stress $\widetilde{\mathbf{U}''_\varphi \mathbf{U}''_\varphi}$ will be denoted $\widetilde{\mathbf{R}}_\varphi$ as the details of the turbulence closure will not be covered here.

$$\begin{aligned}\frac{\partial \alpha_\varphi \overline{\rho}_\varphi \widetilde{\mathbf{U}}_\varphi}{\partial t} + \nabla\bullet(\alpha_\varphi \overline{\rho}_\varphi \widetilde{\mathbf{U}}_\varphi \widetilde{\mathbf{U}}_\varphi) + \nabla\bullet(\alpha_\varphi \overline{\rho}_\varphi \widetilde{\mathbf{R}}_\varphi) + \widehat{\rho\mathbf{U}S_\varphi}\Sigma \\ = -\nabla(\alpha_\varphi \overline{p}_\varphi) + \widehat{\mathbf{n}_\varphi p}\Sigma - \nabla\bullet(\alpha_\varphi \overline{\boldsymbol{\tau}}_\varphi) + \widehat{\mathbf{n}_\varphi\bullet\boldsymbol{\tau}}\Sigma - \alpha_\varphi \overline{\rho}_\varphi \mathbf{g}\end{aligned} \tag{27}$$

The surface averaged correlation terms on the r.h.s. of Eqn. (27) may be decomposed into surface average and surface fluctuation correlations [2] *eg.* $\widehat{\mathbf{n}_\varphi p}\Sigma =$

$\widehat{p}\nabla\alpha_\varphi + \widehat{\mathbf{n}_\varphi p^\sharp}\Sigma$. The first term of this decomposition may then be combined with equivalent conditional mean term in the equation to create a separation between in-phase and surface effects. Applying this to Eqn. (27) gives

$$\frac{\partial\alpha_\varphi\overline{\rho}_\varphi\widetilde{\mathbf{U}}_\varphi}{\partial t} + \nabla\bullet(\alpha_\varphi\overline{\rho}_\varphi\widetilde{\mathbf{U}}_\varphi\widetilde{\mathbf{U}}_\varphi) + \nabla\bullet(\alpha_\varphi\overline{\rho}_\varphi\widetilde{\mathbf{R}}_\varphi) = -\alpha_\varphi\nabla\overline{p}_\varphi - \alpha_\varphi\nabla\bullet\overline{\boldsymbol{\tau}}_\varphi - \alpha_\varphi\overline{\rho}_\varphi\mathbf{g}$$
$$+ (\widehat{p} - \overline{p}_\varphi)\nabla\alpha_\varphi + \nabla\alpha_\varphi\bullet(\widehat{\boldsymbol{\tau}} - \overline{\boldsymbol{\tau}}_\varphi) + \widehat{\mathbf{n}_\varphi p^\sharp}\Sigma + \widehat{\mathbf{n}_\varphi\bullet\boldsymbol{\tau}^\sharp}\Sigma - \widehat{\rho\mathbf{U}S_\varphi}\Sigma. \quad (28)$$

In the work of Hill [4] the interface terms on the r.h.s. of Eqn. (28) are grouped to form the interfacial momentum transfer term from phase φ :

$$\mathbf{M}_\varphi = (\widehat{p} - \overline{p}_\varphi)\nabla\alpha_\varphi + \widehat{\mathbf{n}_\varphi p^\sharp}\Sigma - \widehat{\mathbf{n}_\varphi\bullet\boldsymbol{\tau}}\Sigma \quad (29)$$

and $\mathbf{M}_\varphi$ is subsequently modelled for bubbly flow. It is concluded in [4] that $\mathbf{M}_c = -\mathbf{M}_d$ where the subscripts c and d represent the continuous and dispersed phases respectively. But $\overline{p}_c \neq \overline{p}_d \therefore \mathbf{M}_c \neq -\mathbf{M}_d$ indicating that this particular grouping of terms is not appropriate. However, the approximation applied later in the derivation in which it assumed that the two phase pressures are equal to the phase fraction weighted averaged pressure does ensure that $\mathbf{M}_c = -\mathbf{M}_d$ with $\mathbf{M}_c$ and $\mathbf{M}_d$ defined according to Eqn. (29). This approach also treats the pressure and stress terms inconsistently, which is rather unsatisfactory considering that they are both part of same total stress tensor, the separation into a normal and deviatoric components being done for modelling convenience. Another possible grouping of terms in which both parts of the total stress tensor are treated equivalently is

$$\mathbf{M}_\varphi = (\widehat{p} - \langle p\rangle)\nabla\alpha_\varphi + \nabla\alpha_\varphi\bullet(\widehat{\boldsymbol{\tau}} - \langle\boldsymbol{\tau}\rangle) + \widehat{\mathbf{n}_\varphi p^\sharp}\Sigma + \widehat{\mathbf{n}_\varphi\bullet\boldsymbol{\tau}^\sharp}\Sigma \quad (30)$$

in which $\langle p\rangle$ and $\langle\boldsymbol{\tau}\rangle$ are some kind of averages which combine the values from both phases and are hence the same for both phases. This approach guarantees that $\mathbf{M}_c = -\mathbf{M}_d$ which is essential for the modelling of two-phase flow. Combining Eqs. (28 and 30) results in

$$\frac{\partial\alpha_\varphi\overline{\rho}_\varphi\widetilde{\mathbf{U}}_\varphi}{\partial t} + \nabla\bullet(\alpha_\varphi\overline{\rho}_\varphi\widetilde{\mathbf{U}}_\varphi\widetilde{\mathbf{U}}_\varphi) + \nabla\bullet(\alpha_\varphi\overline{\rho}_\varphi\widetilde{\mathbf{R}}_\varphi) = -\alpha_\varphi\nabla\overline{p}_\varphi - \alpha_\varphi\nabla\bullet\overline{\boldsymbol{\tau}}_\varphi - \alpha_\varphi\overline{\rho}_\varphi\mathbf{g}$$
$$+ (\langle p\rangle - \overline{p}_\varphi)\nabla\alpha_\varphi + \nabla\alpha_\varphi\bullet(\langle\boldsymbol{\tau}\rangle - \overline{\boldsymbol{\tau}}_\varphi) + \mathbf{M}_\varphi - \widehat{\rho\mathbf{U}S_\varphi}\Sigma. \quad (31)$$

Closure of Eqn. (31) requires models for the phase viscous stress tensor $\overline{\boldsymbol{\tau}}_\varphi$, the phase Reynolds stress $\widetilde{\mathbf{R}}_\varphi$, an averaging procedure to obtain $\langle p\rangle$ and $\langle\boldsymbol{\tau}\rangle$ from the phase values, the interfacial momentum transfer rate $\mathbf{M}_\varphi$ and the surface mass transfer term $\widehat{\rho\mathbf{U}S_\varphi}\Sigma$. This is the subject of the next section.

4 Turbulent Two-Phase Flow Equation Closure

It is not necessary to give details of all the modelling necessary to close the conditionally averaged multi-phase equations of the previous section, but those parts which strongly influence the solution algorithm will be described. The first approximation to be applied is that the problems of interest are specifically two-phase rather than multi-phase. This allows some useful equation combinations to be exploited, *eg.* the creation of an equation for the relative velocity between the phases. The greatest numerical difficulty encountered when attempting the solution of Eqn. (31) is the need for a pressure equation for each phase. These equations are elliptic in nature and strongly coupled, requiring some kind of coupled solution procedure. However, in incompressible flow the most important use of the pressure field to force the momentum solution to obey the continuity constraint. If, in two-phase flow, the pressure is used mainly to ensure overall continuity, phase-fraction being guaranteed by the solution of appropriate continuity equations, then only one pressure is required. Clearly this approximation reduces the number of variables in the system by one, which, if the system is to remain well posed, requires the removal of one of the equations. Typically the interface transport equations Eqn. (19) is neglected; the interface distribution being obtained from the continuity equations. Thus a useful approximation (used by most researchers in the field) is to assume that the two phase pressures are equal to the average pressure; but what average? The average commonly used for this purpose is the phase volume fraction mean: $\langle p \rangle = \alpha_b \overline{p}_b + \alpha_a \overline{p}_a$ and this will be used here. Currently the same approximation is applied to the $\nabla\alpha_\varphi \bullet (\langle \boldsymbol{\tau} \rangle - \overline{\boldsymbol{\tau}}_\varphi)$ term, which implies that it is zero, although more realistic modelling approaches have been developed which could be applied. However, it is expected that this term will be small compared with the phase Reynolds stress or interface transfer rate terms and so neglecting it altogether is acceptable and convenient. For the moment interface mass transfer effects are neglected, although it is not expected that serious numerical difficulties will be encountered when they are included. Applying all these approximations to Eqs. (23 and 31) results in

$$\frac{\partial \alpha_\varphi \overline{\rho}_\varphi}{\partial t} + \nabla \bullet (\alpha_\varphi \overline{\rho}_\varphi \widetilde{\mathbf{U}}_\varphi) = 0 \tag{32}$$

and

$$\frac{\partial \alpha_\varphi \overline{\rho}_\varphi \widetilde{\mathbf{U}}_\varphi}{\partial t} + \nabla \bullet (\alpha_\varphi \overline{\rho}_\varphi \widetilde{\mathbf{U}}_\varphi \widetilde{\mathbf{U}}_\varphi) + \nabla \bullet (\alpha_\varphi \overline{\rho}_\varphi \widetilde{\mathbf{R}}_\varphi) = -\alpha_\varphi \nabla \overline{p} - \alpha_\varphi \nabla \bullet \overline{\boldsymbol{\tau}}_\varphi - \alpha_\varphi \overline{\rho}_\varphi \mathbf{g} + \mathbf{M}_\varphi. \tag{33}$$

4.1 Phase Intensive Momentum Equation

A major numerical difficulty is encountered when solving Eqn. (33) in regions where $\alpha_\varphi \to 0$. Various *ad hoc.* numerical tricks could be applied to avoid this

problem, *eg.* limiting α_φ such that $\alpha_\varphi \to \delta$ where $0 < \delta \ll 1$ or by forcing $lim_{\alpha_\varphi \to 0}\widetilde{\mathbf{U}}_\varphi = \widetilde{\mathbf{U}}^*_\varphi$ where $\widetilde{\mathbf{U}}^*_\varphi$ is some limiting value of $\widetilde{\mathbf{U}}_\varphi$ obtained from a model. None of these approaches are satisfactory and it would preferable to be able to solve Eqn. (33) directly even as $\alpha_\varphi \to 0$. This can be achieved if α_φ if factored out of the transport terms in Eqn. (33) and removed by subtracting $\widetilde{\mathbf{U}}_\varphi$ times Eqn. (32) and dividing by $\alpha_\varphi\overline{\rho}_\varphi$. The phase intensive momentum equation obtained by this procedure is

$$\frac{\partial\widetilde{\mathbf{U}}_\varphi}{\partial t} + \widetilde{\mathbf{U}}_\varphi\cdot\nabla\widetilde{\mathbf{U}}_\varphi + \nabla\cdot\widetilde{\mathbf{R}}_\varphi + \frac{\nabla(\alpha_\varphi\overline{\rho}_\varphi)}{\alpha_\varphi\overline{\rho}_\varphi}\cdot\widetilde{\mathbf{R}}_\varphi = -\frac{\nabla\overline{p}}{\overline{\rho}_\varphi} - \frac{\nabla\cdot\overline{\boldsymbol{\tau}}_\varphi}{\overline{\rho}_\varphi} - \mathbf{g} + \frac{\mathbf{M}_\varphi}{\alpha_\varphi\overline{\rho}_\varphi}. \quad (34)$$

Some interesting conclusions can be drawn from the form of Eqn. (34). The first is that

$$\lim_{\alpha_\varphi\to 0}\frac{\mathbf{M}_\varphi}{\alpha_\varphi\overline{\rho}_\varphi} \neq \infty, \quad (35)$$

and must be the case for both phases between which $\mathbf{M}_\varphi$ represents the transfer. For a two-phase system where $\mathbf{M}_a = -\mathbf{M}_b$,

$$\lim_{\alpha_a\to 0}\frac{\mathbf{M}_a}{\alpha_a\overline{\rho}_a} \neq \infty \quad \text{and} \quad \lim_{\alpha_b\to 0}\frac{\mathbf{M}_a}{\alpha_b\overline{\rho}_b} \neq \infty \quad (36)$$

which is a useful constraint on drag and lift modelling for both the dispersed bubble and droplet limits. The second is,

$$\text{given that} \quad \lim_{\alpha_\varphi\to 0}\widetilde{\mathbf{R}}_\varphi \neq \mathbf{0} \quad \text{then} \quad \lim_{\alpha_\varphi\to 0}\frac{\nabla\alpha_\varphi}{\alpha_\varphi} \neq \infty. \quad (37)$$

It is not immediately clear from the equations that this constraint will be obeyed, however, the $\frac{\nabla(\alpha_\varphi\overline{\rho}_\varphi)}{\alpha_\varphi\overline{\rho}_\varphi}\cdot\widetilde{\mathbf{R}}_\varphi$ term in Eqn. (34) produces a divergent phase velocity field which has the effect of dispersing α_φ according to Eqn. (32) which should remove the singularity from the equation. Proof of this has not yet been obtained and further work is required.

4.2 Laminar Stress Modelling

For Newtonian incompressible flow the laminar stress term

$$\frac{\nabla\cdot\overline{\boldsymbol{\tau}}_\varphi}{\overline{\rho}_\varphi} = -\nu_\varphi 2\,\mathrm{dev}(\,\mathrm{symm}(\nabla\widetilde{\mathbf{U}}_\varphi)) \quad (38)$$

$$= -\nu_\varphi(\nabla\widetilde{\mathbf{U}}_\varphi + \nabla\widetilde{\mathbf{U}}_\varphi^T - \frac{2}{3}\mathbf{I}\nabla\cdot\widetilde{\mathbf{U}}_\varphi). \quad (39)$$

4.3 Interfacial Momentum Transfer Modelling

The BRITE II project was predominantly concerned with low phase-fraction dispersed bubbly flow. Under these conditions it is convenient to decompose the interfacial momentum transfer rate into contributions from the bubble drag, lift, virtual mass and Basset forces. The Basset force is very much smaller than the drag and is usually neglected, however, the other three are important and were modelled in the BRITE II project as

$$\begin{aligned} \mathbf{M}_d &= C_d \tfrac{3}{4} \tfrac{\alpha_d \overline{\rho}_c}{d} |\widetilde{\mathbf{U}}_r| \widetilde{\mathbf{U}}_r && \text{drag} \\ &+ C_l \alpha_d \overline{\rho}_c \widetilde{\mathbf{U}}_r \times \nabla \times \widetilde{\mathbf{U}}_c && \text{lift} \\ &+ C_{vm} \alpha_d \overline{\rho}_c \left(\tfrac{D_c \widetilde{\mathbf{U}}_c}{Dt} - \tfrac{D_d \widetilde{\mathbf{U}}_d}{Dt} \right) && \text{virtual mass} \end{aligned} \tag{40}$$

where the relative velocity $\widetilde{\mathbf{U}}_r = \widetilde{\mathbf{U}}_c - \widetilde{\mathbf{U}}_d$. While these models are well posed for low phase-fraction flows, they cannot possibly handle phase inversion or simultaneously the bubble and droplet limits for example. In general, the interfacial momentum transfer rate will have contributions from all the two-phase flow regimes weighted according to probability density functions. Currently not enough is known about two-phase flow to be able to construct such a model so for the purpose of this study the simple mixture model

$$\begin{aligned} \mathbf{M}_a &= \tfrac{3}{4} \alpha_a \alpha_b (\alpha_b \tfrac{C_{d_a} \rho_b}{d_a} + \alpha_a \tfrac{C_{d_b} \rho_a}{d_b}) |\widetilde{\mathbf{U}}_r| \widetilde{\mathbf{U}}_r && \text{drag} \\ &+ \alpha_a \alpha_b (\alpha_b C_{l_a} \rho_b + \alpha_a C_{l_b} \rho_a) \widetilde{\mathbf{U}}_r \times \nabla \times \widetilde{\mathbf{U}} && \text{lift} \\ &+ \alpha_a \alpha_b (\alpha_b C_{vm_a} \rho_b + \alpha_a C_{vm_b} \rho_a) \left(\tfrac{D_b \widetilde{\mathbf{U}}_b}{Dt} - \tfrac{D_a \widetilde{\mathbf{U}}_a}{Dt} \right) && \text{virtual mass} \end{aligned} \tag{41}$$

where

$$\frac{D_a \widetilde{\mathbf{U}}_a}{Dt} = \frac{\partial \widetilde{\mathbf{U}}_a}{\partial t} + \widetilde{\mathbf{U}}_a \cdot \nabla \widetilde{\mathbf{U}}_a \tag{42}$$

and

$$\frac{D_b \widetilde{\mathbf{U}}_b}{Dt} = \frac{\partial \widetilde{\mathbf{U}}_b}{\partial t} + \widetilde{\mathbf{U}}_b \cdot \nabla \widetilde{\mathbf{U}}_b \tag{43}$$

will be used which is capable of realistically (though not accurately) representing the full range of phase fraction. In the limit of $\alpha_a \to 0$ or $\alpha_a \to 1$ Eqn. (41) is equivalent to Eqn. (40), also this model obeys the constraint Eqn. (36) derived in Section 4.1. The lift and virtual mass coefficients in Eqn. (41) are assumed constant and supplied by the user, however, this is not a reasonable assumption for the most important effect: drag. There are many possible drag models (a review is being conducted as part of the BRITE III project) which are valid for different two-phase systems and flow regimes, but for the purposes of this numerical study the simple and reliable solid particle model of Wallis [6] is chosen, which reads

$$C_d = \frac{24}{R_e} \left(1 + 0.15 R_e^{0.687}\right) \qquad R_e \leq 10^3 \tag{44}$$

4.4 Phase Reynolds Stress Modelling

For the purposes of this work the phase Reynolds Stress $\widetilde{\mathbf{R}}_\varphi$ is modelled using the Boussinesq eddy viscosity concept giving

$$\begin{aligned}\widetilde{\mathbf{R}}_\varphi &= -\nu_{t_\varphi} 2\,\mathrm{dev}(\,\mathrm{symm}(\nabla\widetilde{\mathbf{U}}_\varphi)) + \frac{2}{3}\mathbf{I}\widetilde{k}_\varphi \\ &= -\nu_{t_\varphi}(\nabla\widetilde{\mathbf{U}}_\varphi + \nabla\widetilde{\mathbf{U}}_\varphi^T - \frac{2}{3}\mathbf{I}\nabla\cdot\widetilde{\mathbf{U}}_\varphi) + \frac{2}{3}\mathbf{I}\widetilde{k}_\varphi \end{aligned} \tag{45}$$

where

$$\nu_{t_\varphi} = C_\mu \frac{\widetilde{k}_\varphi^2}{\widetilde{\varepsilon}_\varphi}. \tag{46}$$

This model requires the phase turbulent kinetic energy $\widetilde{k}_\varphi$ and dissipation rate $\widetilde{\varepsilon}_\varphi$. In the BRITE II project transport equations were solved for these properties in the continuous phase and an algebraic model used to relate the dispersed phase Reynolds stress to that of the continuous phase. This approach is not completely satisfactory and is unable to handle complex phenomena such as phase inversion which is of particular interest here. However, part of the BRITE III work is to create an appropriate turbulence model for such complex cases and because the issue does not strongly affect the solution algorithm it need not be taken any further here and only laminar cases will be considered. In the expectation that the BRITE III work will again be based on the Boussinesq hypothesis, the momentum equations will retain the Reynolds stress term in this form, which when combined with the laminar stress term gives

$$\begin{aligned}\widetilde{\mathbf{R}}_{eff_\varphi} = \widetilde{\mathbf{R}}_\varphi + \frac{\nabla\cdot\overline{\boldsymbol{\tau}}_\varphi}{\overline{\rho}_\varphi} &= -\nu_{eff_\varphi} 2\,\mathrm{dev}(\,\mathrm{symm}(\nabla\widetilde{\mathbf{U}}_\varphi)) + \frac{2}{3}\mathbf{I}\widetilde{k}_\varphi \\ &= -\nu_{eff_\varphi}(\nabla\widetilde{\mathbf{U}}_\varphi + \nabla\widetilde{\mathbf{U}}_\varphi^T - \frac{2}{3}\mathbf{I}\nabla\cdot\widetilde{\mathbf{U}}_\varphi) + \frac{2}{3}\mathbf{I}\widetilde{k}_\varphi \end{aligned} \tag{47}$$

where the effective viscosity is given by

$$\nu_{eff_\varphi} = \nu_\varphi + \nu_{t_\varphi} \tag{48}$$

5 Incompressible Two-Phase Flow Equations

Some simplification of the equations presented in the previous sections is possible if the two-phase system of interest may be assumed incompressible; in which case the continuity equation Eqn. (32) becomes

$$\frac{\partial\alpha_\varphi}{\partial t} + \nabla\cdot(\overline{\mathbf{U}}_\varphi\alpha_\varphi) = 0 \tag{49}$$

the flows of interest. Considering this, a fairly traditional algorithm is proposed here, capable of handling a wide range of two-phase flow including phase inversion and phase disappearance but not complete separation creating a free surface between the phases. An algorithm which can handle such extreme conditions has been developed and implemented in FOAM and will be described in detail in a subsequent report.

6.1 Discretisation

Equation discretisation is presented in the finite volume notation of Weller [1], a concise, code-independent form which should make it as easy as possible to understand the algorithm and to implement in the code of choice. Currently this notation is still under development and may require significant revision; if any of the terms are not clear or you have any suggestions please contact the author by Email at henry@ic.ac.uk.

6.1.1 Phase-Fraction Equations

Although only one of the phase fraction equations need be solved (the other phase fraction is obtained from $\alpha_b = 1 - \alpha_a$), maintaining boundedness may require the solution of both equations in conjunction with a recombination scheme described in Section 5.1. Discretisation requires the phase-relative fluxes

$$\phi_{r_a} = -\alpha_{b_{f(\phi_r,\Gamma,0.5)}}\phi_r \tag{67}$$

and

$$\phi_{r_b} = \alpha_{a_{f(-\phi_r,\Gamma,0.5)}}\phi_r \tag{68}$$

where

$$\phi_r = \phi_b - \phi_a \tag{69}$$

which are used in the second convection terms the phase-fraction equation pair

$$\left[\!\left[\frac{\partial[\alpha_a]}{\partial t}\right]\!\right] + \left[\!\left[\nabla\bullet\left(\phi[\alpha_a]_{f(\phi,\Gamma,0.5)}\right)\right]\!\right] + \left[\!\left[\nabla\bullet\left(\phi_{r_a}[\alpha_a]_{f(\phi_{r_a},\Gamma,0.5)}\right)\right]\!\right] = 0 \tag{70}$$

and

$$\left[\!\left[\frac{\partial[\alpha_b]}{\partial t}\right]\!\right] + \left[\!\left[\nabla\bullet\left(\phi[\alpha_b]_{f(\phi,\Gamma,0.5)}\right)\right]\!\right] + \left[\!\left[\nabla\bullet\left(\phi_{r_b}[\alpha_b]_{f(\phi_{r_b},\Gamma,0.5)}\right)\right]\!\right] = 0. \tag{71}$$

In order to ensure boundedness, an NVD or TVD scheme should be applied to all convection terms, the example here is the Γ scheme [9] used in TVD mode. Upwind differencing could be applied if first-order accuracy is adequate. Note carefully the sign of the fluxes used to interpolate the phase fractions in the relative fluxes; this ensures the two equations are numerically equivalent *i.e.* $\alpha_b = 1 - \alpha_a$ even if both equations are solved, and the boundedness is guaranteed at both limits.

(63) is also conservative and $0 \leqslant \alpha_a \leqslant 1$ because the term becomes zero at both limits. An interesting and useful feature of this approach is that the α_a and α_b equations have the same form

$$\frac{\partial \alpha_b}{\partial t} + \nabla\cdot(\overline{\mathbf{U}}\alpha_b) + \nabla\cdot(\overline{\mathbf{U}}_r\alpha_b(1-\alpha_b)) = 0. \tag{64}$$

The problem with this approach is that boundedness at both limits can only be guaranteed if the equation is solved fully implicitly, but the second convection term is non-linear in α_a so the use of a linear solver will require an iterative procedure to correct for the non-linearity. Such procedures are not guaranteed to be convergent, particularly if, in this case, slight unboundedness is generated during the iterations. Convergence of the iterative procedure may be accelerated by solving both Eqs. (63 and 64) and blending α_a and α_b to ensure $0 \leqslant \alpha_a \leqslant 1$, *eg.*

$$\alpha_a^* = \frac{\alpha_a}{\alpha_a + \alpha_b}. \tag{65}$$

which only corrects the upper limit (the lower limit should not be violated because it is handled implicitly), or

$$\alpha_a^* = \frac{1}{2}(1 - (1-\alpha_a)^2 + (1-\alpha_b)^2) \tag{66}$$

which removes unboundedness at both limits. These methods should only be used during the iterations and not after the final iteration otherwise some small level of conservation error may result.

6 Two-Phase Flow Equation Solution

The system of equations for incompressible turbulent two-phase flow Eqs. (63, 57, 58 and 49) is complete, closed and susceptible to numerical solution. The need to obey the incompressibility constraint Eqn. (49) implies that a pressure equation based solution algorithm would be most appropriate. For steady-state problems SIMPLE [7] or one of the variants could be used (as in the BRITE II project) or PISO [8] for transient runs; in either case a pressure equations is constructed from the discretised momentum equations Eqs. (63 and 57) and the incompressibility constraint Eqn. (49). Industrial two-phase flow typically occurs in complex geometries for which unstructured collocated computational meshes are most appropriate. However, difficulties arise in handling large density gradients, caused by *eg.* complete phase separation, on such meshes (problems not encountered on staggered structured meshes) which require special interpolation practices. Implementation of these interpolation practices in traditional industrial CFD codes may cause some difficulty but may not be important for

and

$$\frac{\partial \overline{\mathbf{U}}_b}{\partial t} + \overline{\mathbf{U}}_b^{\mathcal{T}} \bullet \nabla \overline{\mathbf{U}}_b - \nabla \bullet (\nu_{eff_b} \nabla \overline{\mathbf{U}}_b) + \nabla \bullet \overline{\mathbf{R}}_{eff_b}^{\mathcal{C}} + \frac{\nabla \alpha_b}{\alpha_b} \bullet \overline{\mathbf{R}}_{t_b}^{\mathcal{C}}$$
$$= -\frac{\nabla \overline{p}}{\rho_b} - \mathbf{g} - \frac{\alpha_b}{\rho_b} \left(A_d(\overline{\mathbf{U}}_b - \overline{\mathbf{U}}_a) + A_l + A_{vm} \left(\frac{D_b \overline{\mathbf{U}}_b}{Dt} - \frac{D_a \overline{\mathbf{U}}_a}{Dt} \right) \right) \quad (58)$$

where

$$\begin{array}{lcll} A_d & = & \frac{3}{4}(\alpha_b \frac{C_{d_a} \rho_b}{d_a} + \alpha_a \frac{C_{d_b} \rho_a}{d_b}) |\overline{\mathbf{U}}_r| & \text{drag} \\ A_l & = & (\alpha_b C_{l_a} \rho_b + \alpha_a C_{l_b} \rho_a) \overline{\mathbf{U}}_r \times \nabla \times \overline{\mathbf{U}} & \text{lift} \\ A_{vm} & = & \alpha_b C_{vm_a} \rho_b + \alpha_a C_{vm_b} \rho_a & \text{virtual mass.} \end{array} \quad (59)$$

5.1 Phase-Fraction Boundedness

A key issue in the numerics of two-phase flow is the boundedness of the phase-fraction. If one attempts to solve Eqn. (49) in this form, applying an appropriate bounded discretisation scheme, then the constraint $\alpha_\varphi \geqslant 0$ will be obeyed but the constraint $\alpha_\varphi \leqslant 1$ may not be. However, if one solves both for $\alpha_a \geqslant 0$ and $\alpha_b \geqslant 0$ then it would be possible, by suitable blending, to obtain a value of α_φ which obeys both constraints; this value will of course not necessarily obey the equations and may not be conservative. This approach is therefore unacceptable as phase conservation is a critical issue in multi-phase flow with high density ratios because small volume-fraction errors may correspond to large mass-fraction errors. A better approach would be to rearrange Eqn. (49) such that a numerical approach may be applied which is bounded at both extremes of the phase-fraction range. One possibility is to decompose $\overline{\mathbf{U}}_a$ into the mean and relative parts

$$\overline{\mathbf{U}}_a = \overline{\mathbf{U}} - \alpha_b \overline{\mathbf{U}}_r \quad (60)$$

where

$$\overline{\mathbf{U}}_r = \overline{\mathbf{U}}_a - \overline{\mathbf{U}}_b \quad (61)$$

and

$$\overline{\mathbf{U}} = \alpha_a \overline{\mathbf{U}}_a + \alpha_b \overline{\mathbf{U}}_b. \quad (62)$$

Substituting Eqn. (60) into Eqn. (49) gives

$$\frac{\partial \alpha_a}{\partial t} + \nabla \bullet (\overline{\mathbf{U}} \alpha_a) - \nabla \bullet (\overline{\mathbf{U}}_r \alpha_a (1 - \alpha_a)) = 0. \quad (63)$$

The first convection term in Eqn. (63) is conservative and $0 \leqslant \alpha_a \leqslant 1$ because $\nabla \bullet \overline{\mathbf{U}} = 0$ (*cf.* Eqn. (51)) which means it is equivalent to $\overline{\mathbf{U}} \bullet \nabla \alpha_a$ which is an amplitude preserving wave transport term. The second convection term in Eqn.

and the phase intensive momentum equation Eqn. (34) becomes

$$\frac{\partial \overline{\mathbf{U}}_\varphi}{\partial t} + \overline{\mathbf{U}}_\varphi \cdot \nabla \overline{\mathbf{U}}_\varphi + \nabla \cdot \overline{\mathbf{R}}_{eff_\varphi} + \frac{\nabla \alpha_\varphi}{\alpha_\varphi} \cdot \overline{\mathbf{R}}_\varphi = -\frac{\nabla \overline{p}}{\rho_\varphi} - \mathbf{g} + \frac{\mathbf{M}_\varphi}{\alpha_\varphi \rho_\varphi}. \tag{50}$$

Combining Eqn. (49) for both phases a and b demonstrates the incompressibility constraint

$$\nabla \cdot \overline{\mathbf{U}} = 0 \tag{51}$$

where $\overline{\mathbf{U}} = \alpha_a \overline{\mathbf{U}}_a + \alpha_b \overline{\mathbf{U}}_b$.

For numerical implementation of Eqn. (50) it is useful to decompose the Reynolds stress terms into a diffusive component and a correction $\overline{\mathbf{R}}_{eff_\varphi} = \overline{\mathbf{R}}_\varphi^{\mathcal{D}} + \overline{\mathbf{R}}_\varphi^{\mathcal{C}}$ where

$$\overline{\mathbf{R}}_\varphi^{\mathcal{D}} = -\nu_{eff_\varphi} \nabla \overline{\mathbf{U}}_\varphi \tag{52}$$

and

$$\overline{\mathbf{R}}_\varphi^{\mathcal{C}} = \overline{\mathbf{R}}_{eff_\varphi} + \nu_{eff_\varphi} \nabla \overline{\mathbf{U}}_\varphi \tag{53}$$

Modelling the Reynolds stress according to the Boussinesq eddy viscosity hypothesis Eqn. (47) leads to a Reynolds stress correction term of the form

$$\overline{\mathbf{R}}_{eff_\varphi}^{\mathcal{C}} = -\nu_{eff_\varphi} (\nabla \overline{\mathbf{U}}_\varphi{}^T - \frac{2}{3} \mathbf{I} \nabla \cdot \overline{\mathbf{U}}_\varphi) + \frac{2}{3} \mathbf{I} \overline{k}_\varphi. \tag{54}$$

which, when substituted into Eqn. (50), gives

$$\frac{\partial \overline{\mathbf{U}}_\varphi}{\partial t} + \overline{\mathbf{U}}_\varphi \cdot \nabla \overline{\mathbf{U}}_\varphi - \nabla \cdot (\nu_{eff_\varphi} \nabla \overline{\mathbf{U}}_\varphi) + \nabla \cdot \overline{\mathbf{R}}_{eff_\varphi}^{\mathcal{C}} - \nu_{t_\varphi} \frac{\nabla \alpha_\varphi}{\alpha_\varphi} \cdot \nabla \overline{\mathbf{U}}_\varphi + \frac{\nabla \alpha_\varphi}{\alpha_\varphi} \cdot \overline{\mathbf{R}}_{t_\varphi}^{\mathcal{C}} = -\frac{\nabla \overline{p}}{\rho_\varphi} - \mathbf{g} + \frac{\mathbf{M}_\varphi}{\alpha_\varphi \rho_\varphi}. \tag{55}$$

The two convection terms may be combined by defining a total phase velocity

$$\overline{\mathbf{U}}_\varphi^{\mathcal{T}} = \overline{\mathbf{U}}_\varphi - \nu_{t_\varphi} \frac{\nabla \alpha_\varphi}{\alpha_\varphi} \tag{56}$$

which includes both in-phase and interface transport effects which, when substituted into Eqn. (55) together with Eqn. (41) gives

$$\frac{\partial \overline{\mathbf{U}}_a}{\partial t} + \overline{\mathbf{U}}_a^{\mathcal{T}} \cdot \nabla \overline{\mathbf{U}}_a - \nabla \cdot (\nu_{eff_a} \nabla \overline{\mathbf{U}}_a) + \nabla \cdot \overline{\mathbf{R}}_{eff_a}^{\mathcal{C}} + \frac{\nabla \alpha_a}{\alpha_a} \cdot \overline{\mathbf{R}}_{t_a}^{\mathcal{C}} = -\frac{\nabla \overline{p}}{\rho_a} - \mathbf{g} + \frac{\alpha_b}{\rho_a} \left(A_d (\overline{\mathbf{U}}_b - \overline{\mathbf{U}}_a) + A_l + A_{vm} \left(\frac{D_b \overline{\mathbf{U}}_b}{Dt} - \frac{D_a \overline{\mathbf{U}}_a}{Dt} \right) \right) \tag{57}$$

6.1.2 Phase-Momentum Equations

The total convection fluxes of momentum, including in-phase convection and interface transport effects, are

$$\phi_a^{\mathcal{T}} = \phi_a - \nu_{t_{af}} \frac{S_f \nabla_f^{\perp} \alpha_a}{\alpha_{af} + \delta} \tag{72}$$

and

$$\phi_b^{\mathcal{T}} = \phi_b - \nu_{t_{bf}} \frac{S_f \nabla_f^{\perp} \alpha_b}{\alpha_{bf} + \delta}. \tag{73}$$

The momentum equations are discretised in the decoupled semi-implicit form

$$\begin{aligned}
&\left[\!\left[\frac{\partial[\overline{\mathbf{U}}_a]}{\partial t}\right]\!\right] + \left[\!\left[\nabla\!\bullet\!\left(\phi_a^{\mathcal{T}}[\overline{\mathbf{U}}_a]_{f(\phi_a^{\mathcal{T}},\mathrm{UD},)}\right)\right]\!\right] - \left[\!\left[\nabla\!\bullet\!\left(\phi_a^{\mathcal{T}}\right)[\overline{\mathbf{U}}_a]\right]\!\right] - \left[\nabla\!\bullet\!\left(\nu_{eff_a}\nabla[\overline{\mathbf{U}}_a]\right)\right] \\
&\qquad + \nabla\!\bullet\!\overline{\mathbf{R}}_{eff_a}^{\mathcal{C}} + \frac{\nabla\alpha_a}{\langle\alpha_a\rangle_{\nabla} + \delta}\!\bullet\!\overline{\mathbf{R}}_{t_a}^{\mathcal{C}} = -\frac{\nabla\overline{p}}{\rho_a} - \mathbf{g} \\
&- \left[\!\left[\frac{\alpha_b}{\rho_a} A_d[\overline{\mathbf{U}}_a]\right]\!\right] - \frac{\alpha_b}{\rho_a} A_{vm}\left[\!\left[\frac{D_a[\overline{\mathbf{U}}_a]}{Dt}\right]\!\right] + \frac{\alpha_b}{\rho_a}\left(A_d\overline{\mathbf{U}}_b + A_l + A_{vm}\frac{D_b\overline{\mathbf{U}}_b}{Dt}\right)
\end{aligned} \tag{74}$$

and

$$\begin{aligned}
&\left[\!\left[\frac{\partial[\overline{\mathbf{U}}_b]}{\partial t}\right]\!\right] + \left[\!\left[\nabla\!\bullet\!\left(\phi_b^{\mathcal{T}}[\overline{\mathbf{U}}_b]_{f(\phi_b^{\mathcal{T}},\mathrm{UD},)}\right)\right]\!\right] - \left[\!\left[\nabla\!\bullet\!\left(\phi_b^{\mathcal{T}}\right)[\overline{\mathbf{U}}_b]\right]\!\right] - \left[\nabla\!\bullet\!\left(\nu_{eff_b}\nabla[\overline{\mathbf{U}}_b]\right)\right] \\
&\qquad + \nabla\!\bullet\!\overline{\mathbf{R}}_{eff_b}^{\mathcal{C}} + \frac{\nabla\alpha_b}{\langle\alpha_b\rangle_{\nabla} + \delta}\!\bullet\!\overline{\mathbf{R}}_{t_b}^{\mathcal{C}} = -\frac{\nabla\overline{p}}{\rho_b} - \mathbf{g} \\
&- \left[\!\left[\frac{\alpha_a}{\rho_b} A_d[\overline{\mathbf{U}}_b]\right]\!\right] - \frac{\alpha_a}{\rho_b} A_{vm}\left[\!\left[\frac{D_b[\overline{\mathbf{U}}_b]}{Dt}\right]\!\right] + \frac{\alpha_a}{\rho_b}\left(A_d\overline{\mathbf{U}}_a + A_l + A_{vm}\frac{D_a\overline{\mathbf{U}}_a}{Dt}\right).
\end{aligned} \tag{75}$$

The time derivative, convection and diffusion terms are handled implicitly, the Reynolds stress correction, pressure gradient, buoyancy and lift terms are handled explicitly and the drag and virtual mass terms handled semi-implicitly by making the part involving the velocity being solved for implicit and other part explicit. This discretisation approach has proved very stable in both transient and steady state modes; the complex partial-eliminations procedures of the BRITE II project [4] have not proved beneficial in the tests conducted in FOAM. For the construction of the pressure equation, the momentum matrices are stored without the pressure gradient term such that

$$[\mathcal{M}_a[\mathbf{U}_a]] = -\frac{\nabla\overline{p}}{\rho_a} \tag{76}$$

and

$$[\mathcal{M}_b[\mathbf{U}_b]] = -\frac{\nabla\overline{p}}{\rho_b}. \tag{77}$$

6.1.3 Phase-Momentum Correction Equations

The phase-momentum correction equations are obtained by decomposing the matrixes in Eqs. (76 and 77) into diagonal and 'H' parts and rearranging, giving

$$\overline{\mathbf{U}}_a = \frac{\mathbf{H}_a}{A_a} - \frac{\nabla \overline{p}}{\rho_a A_a} \tag{78}$$

and

$$\overline{\mathbf{U}}_b = \frac{\mathbf{H}_b}{A_b} - \frac{\nabla \overline{p}}{\rho_a A_b} \tag{79}$$

where

$$A_a = [\mathcal{M}_a[\mathbf{U}_a]]_D, \qquad \mathbf{H}_a = [\mathcal{M}_a[\mathbf{U}_a]]_H \tag{80}$$

and

$$A_b = [\mathcal{M}_b[\mathbf{U}_b]]_D, \qquad \mathbf{H}_b = [\mathcal{M}_b[\mathbf{U}_b]]_H \tag{81}$$

(82)

6.1.4 Pressure Equation

Equations for the face volumetric fluxes are created by interpolating the momentum correction equations Eqs. (78 and 79) using central differencing giving

$$\phi_a = \phi_a^* - \left(\frac{1}{\rho_a A_a}\right)_f S_f \nabla_f^{\perp} \overline{p} \tag{83}$$

and

$$\phi_b = \phi_b^* - \left(\frac{1}{\rho_b A_b}\right)_f S_f \nabla_f^{\perp} \overline{p} \tag{84}$$

where the flux predictions are given by

$$\phi_a^* = \left(\frac{\mathbf{H}_a}{A_a}\right)_f \bullet \mathbf{S}_f \tag{85}$$

and

$$\phi_b^* = \left(\frac{\mathbf{H}_b}{A_b}\right)_f \bullet \mathbf{S}_f \tag{86}$$

Given that the total face volumetric flux is given by

$$\phi = \alpha_{af}\phi_a + \alpha_{bf}\phi_b \tag{87}$$

and the continuity constraint may be written

$$\nabla \bullet (\phi) = 0 \tag{88}$$

the pressure equation is constructed by substituting Eqs. (85, 86 and 87) into Eqn. (88) giving

$$\left[\!\left[\nabla\bullet\left(\left(\alpha_{af}\left(\frac{1}{\rho_a A_a}\right)_f+\alpha_{bf}\left(\frac{1}{\rho_b A_b}\right)_f\right)\nabla[\overline{p}]\right)\right]\!\right]=\nabla\bullet(\alpha_{af}\phi_a^*+\alpha_{bf}\phi_b^*). \tag{89}$$

After the pressure solution the fluxes are corrected using Eqs. (83 and 84).

6.1.5 Substantive derivatives

After the PISO loop the substantive derivatives are corrected using

$$\frac{D_a\overline{\mathbf{U}}_a}{Dt}=\frac{\partial\overline{\mathbf{U}}_a}{\partial t}+\nabla\bullet\left(\phi_a\overline{\mathbf{U}}_{af(\phi_a,\Gamma,0.5)}\right)-\nabla\bullet\left(\phi_a\right)\overline{\mathbf{U}}_a \tag{90}$$

$$\frac{D_b\overline{\mathbf{U}}_b}{Dt}=\frac{\partial\overline{\mathbf{U}}_b}{\partial t}+\nabla\bullet\left(\phi_b\overline{\mathbf{U}}_{bf(\phi_b,\Gamma,0.5)}\right)-\nabla\bullet\left(\phi_b\right)\overline{\mathbf{U}}_b \tag{91}$$

6.2 Solution Algorithm

The solution algorithm used PISO to handle the pressure-velocity coupling which requires a momentum predictor and a correction loop in which the pressure equation is solved and the momentum corrected based on the pressure change. The phase-fraction is solved only once per time step before the momentum predictor. For most cases solving only for the dispersed phase-fraction has proved adequate but for cases with strong phase-inversion in which there are significant regions where the nominally continuous phase has a very low phase fraction it may be advantageous to solve for both in an iterative sequence, correcting for unboundedness after each iteration.

1. Optional α-Loop:
   (a) Solve the α_a-equation, Eqn. (70).
   (b) Solve the α_b-equation, Eqn. (71).
   (c) Bound α_a and α_b using Eqn. (65) or Eqn. (66).
2. Solve the α_a-equation, Eqn. (70).
3. Calculate coefficients A_d, A_l and A_{vm}, Eqn. (59).
4. Construct and solve the momentum equations, Eqs. (74 and 75).
5. PISO-Loop:
   (a) Predict fluxes using Eqs. (85 and 86).
   (b) Construct and solve the pressure equation Eqn. (89).

(c) Correct fluxes using Eqs. (83, 84 and 87).

(d) Correct velocities using Eqs. (78 and 79).

6. Correct the convective derivatives using Eqs. (90 and 91)

7. Solve $k - \epsilon$ equations (if required).

7 Conclusion

The two-phase flow algorithm presented in this report is the result of an intensive research effort using FOAM. Careful consideration of the failings of the BRITE II algorithm has lead to a new set of practices designed to create a more general and robust approach. In particular, the problems in solving for the phase velocities in the limit of the phase-fractions going to zero is remedied by creating a phase-intensive form of the equations by decomposing terms and dividing by the phase fractions. This approach requires that the phase-fractions be bounded and conservative which is achieved by a novel splitting of the convection term in the phase-fraction equation and the application of appropriate discretisation practices. This new algorithm is capable of handling the full range of phase-fraction, phase-inversion and local phase-separation but only for modest density ratios. If phase separation at large density ratios occurs, *eg.* the free surface in a bubble-column, then a more complex pressure interpolation practice is required; this is the subject of a subsequent report. A FOAM code containing this algorithm will be supplied with pre-run test cases and documentation.

References

[1] Weller, H.G.: "A Code Independent Notation for Finite Volume Algorithms", Technical report, Imperial College of Science, Technology and Medicine, July 1999.

[2] Weller, H.G.: "The Development of a New Flame Area Combustion Model Using Conditional Averaging", Thermo-Fluids Section Report TF 9307, Imperial College of Science, Technology and Medicine, March 1993.

[3] Dopazo, C.: "On conditional averages for intermittent turbulent flows", *J. Fluid Mech.*, 81:433–438, 1977.

[4] Hill, D.P.: *The Computer Simulation of Dispersed Two-Phase Flow*, PhD thesis, Imperial College of Science, Technology and Medicine, 1998.

[5] Candel, S.M. and Poinsot, T.J.: "Flame Stretch and the Balance Equation for Flame Area", *Combust. Sci. and Tech*, 70:1–15, 1990.

[6] Wallis, G.B.: *One Dimensional Two-phase Flow*: McGraw Hill, New York, 1969.

[7] Patankar, S.V. and Spalding, D.B.: "A Calculation Procedure for Heat, Mass and Momentum Transfer in 3-d parabolic Flow", *Int. J. of Heat and Mass Transfer*, 15:1787, 1972.

[8] Issa, R.I.: "Solution of the Implicitly Discretised Fluid Flow Equations by Operator-Splitting", *J. Comp. Phys.*, 62(1):40–65, January 1986.

[9] Jasak, H., Weller, H.G., and Gosman, A.D.: "High Resolution NVD Differencing Scheme for Arbitrarily Unstructured Meshes", *Int. J. for Numerical Methods in Fluids*, 1999: To be published.

BRITE/EuRam BE-4322

Development of a Computational Code for the Design of Multi-Phase Processes at High Phase Fraction

6-month Report #1

July 8, 1998

1 Technical Overview.

1.1 Summary of Specific Objectives

Work for this 6-month period was scheduled to be on Sub-Tasks 1.1 (INPT), 1.2 & 1.3 (IC), 2.2 (TU Delft), 2.3 (Unilever URV) and 3.1 (IC, CD). No tasks were scheduled for ICI or Total for this 6-month period.

1.2 Technical Progress Report.

Sub-Task 1.1. Model Experiments (INPT)

The contribution of INPT/LGC/IMFT in the BRITE project concerns the experimental investigation of turbulent bubbly flows and liquid-liquid flows at high phase ratio. Experiments have been required to understand the turbulent flow induced in the liquid by high void fraction, hold-up distribution and large scale structures. Two types of experimental studies in simple flow geometries have been proposed :

- Experiment A (A1 & A2) : homogeneous isotropic turbulence flow (fluidized bed)
- Experiment B (B1 & B2): shear turbulence flow (mixing layer)

The following summarizes the work progress related to experiment B only.

a) Experiment B1 : gas-liquid system

The proposed modifications of the existing gas-liquid mixing layer facility to ensure the production of calibrated bubbles at the flow inlet were not possible. The existing facility was too old and too large for the correct injection of a large amount of bubbles. It was decided to build a new, smaller experimental device. The new experiment consists of plane vertical mixing layers generated by two co-current dispersed flows. Each stream is supplied separately. The bulk velocities and the dispersed phase volume fraction (void fraction) can be easily adjusted, so the facility allows the control of the shear ratio and the level of turbulence of the liquid phase, together with the influence of the dispersed phase. The new facility (IMFT) consists of a vertical channel of 3 m height and 0.15×0.3 m^2 cross area where the mixing layers develop from bottom to the top (figure 1). The channel is supplied at bottom by an inlet feeder consisting of a large water tank (1 m $\times$ 1 m $\times$ 0.8 m), inox screens and a convergent section (18 : 1 ratio, 0.9 m height) divided into two parts by a vertical splitter plate of 2 mm thickness. Each part is supplied independently by a bubbly flow of given air and water rates. The water flow is provided by an existing constant level tank at a height of more than 20 m. The water velocities of each flow, at the inlet of the channel, can be adjusted between 0 and 1 ms^{-1}. At the channel outlet, water is collected in a large upper reservoir, and gravity-fed into a lower reservoir. Air bubbles are injected into the channel just after the convergent section. For each stream, the bubble injectors consist of 625 long inox-needles of 0.9 m length, 1 mm external diameter and 0.3 mm inner diameter. They are supplied by two inox-boxes of 0.15×0.15 m^2 and 0.15 m height, covered by two perforated plates to allow the feeding of the needles. The pressure loss caused by the needles will ensure a uniform air injection. Quite uniform bubble diameters are expected for a fixed void fraction, but it will be possible that the bubble sizes will increase slightly with increased void-fraction. Calibrated rotameters are used for air mass flow rates. The void fraction is expected to be up to 25%. The test

section will be equipped with a traversing mechanism allowing the displacement of the measuring probes in the (x, y) vertical plane.

Image processing applied to bubbly flow has been developed to analyse the dynamics of the dispersed phase. For signal processing development, a plane bubbly plume was selected as a test flow, with dimensions similar to the mixing layer to be studied. We have first focused on the lighting system. With ordinary light it is possible to study the dynamics of the frontier of the bubbly flow. In a plane bubbly plume strong instabilities are illuminated. The frequency and the wave numbers of the flapping behavior of the plume were estimated and successfully compared to optical fiber probe measurements. In another approach, we are trying to high speed video record the bubbly plume with a laser sheet. This should help us to analyse the core region of the flow, and its spatial and temporal structure.

The next step is to finish building the new experimental facility and the traversing mechanism for the measurement probes. Then we have to observe the main characteristics of the flows. The final product of this preliminary study will be a two-phase flow chart describing the different flow regimes identified and the range of flow parameters that have to be investigated. Visualizations of both bubbly and drop flows will be performed in order to identify the flow regimes at high phase fraction for which the measuring techniques developed can be applied. More specifically, the objectives are to detect low frequency instabilities in the flows and the flow regimes in which excessive breakage or coalescence rates make analysis of the local hydrodynamic field difficult. Concerning the experimental program, we will first increase slightly the void fraction in order to determine the critical value where the presence of bubbles mainly changes the structure of the flow in the liquid phase. Then local experimental investigations at high void fraction will take place. The heart of our experimental work will be the local analysis of the flow structure in both phases by means of optical probes while hot film anemometry will be used for liquid phase velocity measurements.

b) Experiment B2 : Liquid-liquid system

The experimental set-up is shown in figure 2 The mixing layer is realized in a rectangular column (0.1 m $\times$ 0.2 m $\times$ 2 m), made with glass walls. Each part of the continuous flow is fed independently, and each flow rate can be adjusted. The dispersed phase is injected in the mixing layer after a convergent section by 900 capillary tubes, in order to obtain 2 mm in diameter drops (according with the choice of the phases presented bellow). These 0.35 m long tubes have an internal diameter of 1 mm and an external one of 2.5 mm. The terminal velocity of such drops is about 0.1 ms^{-1}. The experimental set-up is designed for maximum flow rates of 5 m^3hr^{-1} for the continuous phase and 4 m^3hr^{-1} for the dispersed one. A 0.35 m^3 gravity settler is used to separate the phases before recycling. The phases are directly pumped from the settler.

The choice of liquid-liquid systems is dictated by the experimental technique, based upon refractive index matching of the phases. Water is chosen as the continuous phase because of its solvent power (another component has to be added for refractive index matching) and in order to compare the results for liquid-liquid system with the ones obtained for gas-liquid system. For the dispersed phase an organic phase is used. The dispersed phase has to coalesce relatively easily to perform separation of the phases at the duct outlet, but coalescence has to be avoided in the mixing layer. Furthermore, this organic phase must be non toxic and, of course, immiscible with water. Its refractive index must be close enough to the one of water to allow optical matching. For all these reasons,

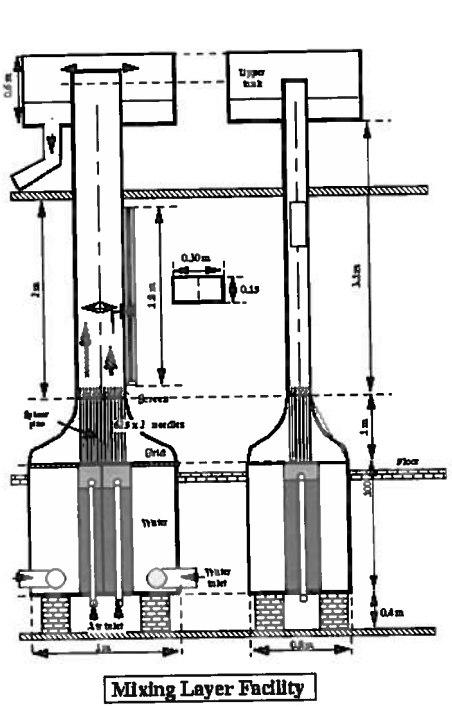

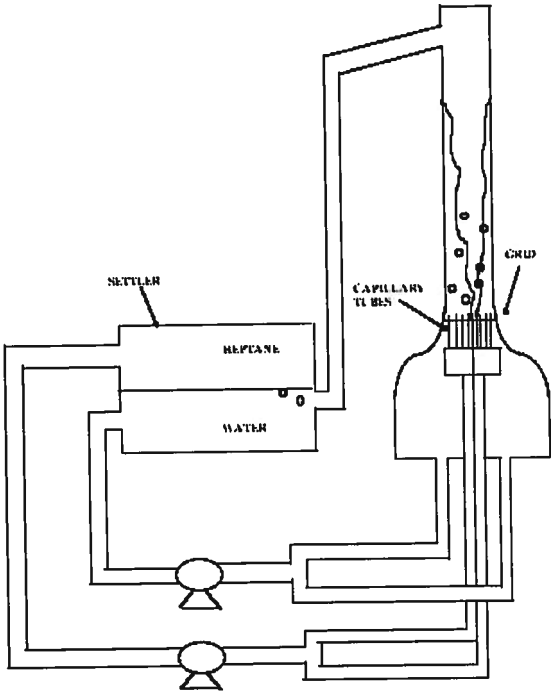

Figure 1: (Left). New experimental facility for experiment B1.

Figure 2: (Right). Experimental setup for experiment B2.

heptane has been chosen ($n_D = 1.385$ for heptane and 1.338 for water). Refractive indices are matched by addition of dextrose ($C_6H_{12}O_6$) in water. This componant is not miscible with heptane. Refractive indices are matched for 37% in weight of dextrose in water at $25°C$. The figure 3 shows the variation of the refractive index of dextrose in water solutions versus temperature for different dextrose fractions.

Measurement technique.

A laser sheet illuminates the flow without refraction on the dispersed phase because of the optical matching. However, the two phases are maintained discernible thanks to a fluorescent tracer present in the continuous phase. According with the wavelength of the laser used, rhodamine B has been chosen as the fluoresent tracer. Moreover, rhodamine B is only miscible in the water phase. A high resolution camera films the plane illuminated inside the flow. The instataneous velocity fields of the continuous phase are computed from the displacements of seeded particles between two consecutive images, the same type of treatment can be applied to the droplets displacements. By statistical treatment, it is then possible to determine mean velocities, rms velocities. The hold-up is computed by image analysis. The major part of the measurement equipment has been already acquired, and the technique is under development. This development can be considered as the main goal for the next months.

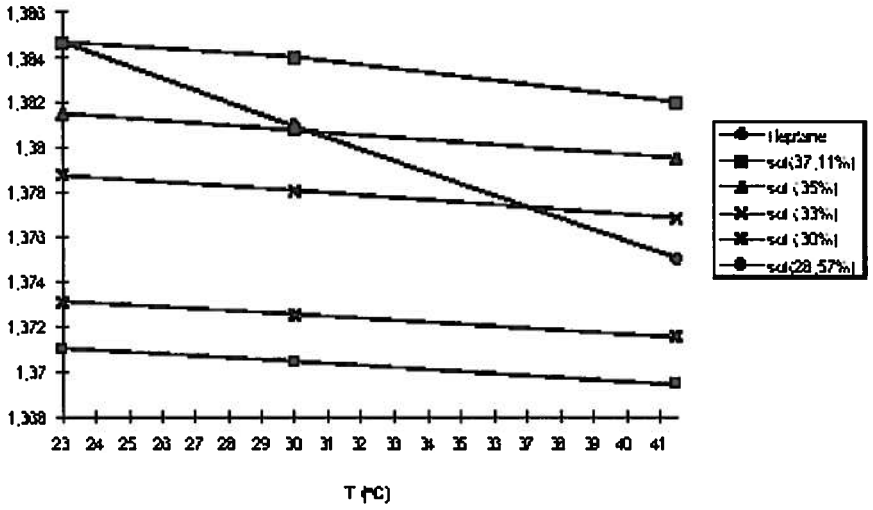

Figure 3: Variation of the refractive index of dextrose in water solution versus temperature for different dextrose fractions.

Sub-Task 1.2. Dynamics of Two-Phase Flow at High Volume Fraction. (IC)

The objective here is to extend the modelling used in BRITE-II to higher phase fractions, where distortion of the dispersed phase (bubbles or droplets) and inter-particle interactions are likely to be of importance. A literature survey to determine what modelling is available has been undertaken ; however very little further modelling has been unearthed, so it seems likely that the project will rely on fundamental research work done by IC in collaboration with the other partners. At IC we have access to a body of work on volume methods for directly simulating bubble or droplet dynamics[1]. These use interface capturing methods to simulate the motion of the interface between the bubble (or droplet) and the surrounding fluid, including interface effects such as surface tension. Numerical experiments involving such techniques will be used to investigate the detailed behaviour of bubbles and droplets in various building-block flows such as shear flow, and the effect of inter-particle interactions on drag, lift, etc.

Potentially at high phase fractions, the two-fluid formulation may be inappropriate. Some theoretical work has been undertaken (linked with the work for Sub-Task 3.1) to investigate alternative formulations of the equations to use in these circumstances. In particular, a mixture model approach, in which transport equations for the combined fluid are formulated and solved, may be appropriate.

Sub-Task 1.3. Turbulence Modelling at High Volume Fraction. (IC)

Work has only just begun on this subtask, commencing with a literature review being undertaken. Again, it seems unlikely that there is much existing work on modelling that can be used, so much of the modelling will have to be generated within the project. One approach which may be very useful is numerical experimentation, using DNS or LES of bubble-turbulence interaction and the interface capturing techniques described above. This can be used to investigate the interactions between small groups of bubbles and turbulence, at medium and high phase fraction. However such calculations are computationally expensive, and so much thought will go into the types of questions to be answered. The exact implementation of the turbulence modelling will depend on the form of the equations being solved, so work on subtask 3.1 must proceed further before this becomes an issue. However one approach being considered is to replace the current C_t modelling, instead solving a separate pde system for the turbulence in each phase. This allows history and transport effects to be included in the dispersed phase turbulence system.

Sub-Task 2.2. Modelling of Breakup and Coalsescence at High Phase Fraction. (TU Delft)

Breakup phenomena in concentrated emulsions

The objective of this sub-project is to develop scaling rules for breakup in liquid/liquid systems at high phase concentrations. The ultimate goal is to derive expressions for the breakup probability and breakup time, both as a function of droplet size, shear rate, viscosity ratio and volume fraction.

In order to obtain these results we intend to :

1. Construct an apparatus suitable for studying breakup phenomena
2. Find a liquid/liquid system in which breakup of concentrated emulsions can be visualized
3. Perform measurements by increasing the shear rate until breakup occurs and record droplet size, shear rate at break and time for breakup.
4. Evalute all measurement data and derive scaling rules

The construction of the apparatus (a counter rotating Coutte instrument, denoted as 'Rheoscope') proceeds well. All parts are ready for assembly. After that, the apparatus and control program will be tested. The liquid/liquid system must be such that a single droplet inside a concentrated emulsion can be studied. This can be achieved by starting with a system in which the aqueous and the oil components have identical refracive indices and light scattering is prevented. A single, coloured droplet placed inside this system can then be observed without difficulty. An optically matched system was found by choosing silicon oil as the oil phase and a 50% glycerol/water mixture as the aqueous phase. The system was stabilized by adding SDS (Sodium Dodecyl Sulfanate) or Dobanol 91-8 surfactant. Two problems remain. Firstly, the system is not density matched and the aqueous phase tends to collect at the bottom of the test tubes. This could be overcome by

adding halogenated solvents (TetraChloroEthylene or TetraBromoEthylene) to the silicon oil. However, because of the high toxity of these substances it is preferable to try and find other ways. The second problem is the couloring of the remaining droplet. All common colorants dissolve better in water than in oil and tend to leak consideraby during the timescale of a measurement. At this moment the best candidate for a colorant seems to be Sudan Red.

Coalescence in shear flow at high volume fractions

A review has been done of experimental and theoretical work concerning efficiency and collision frequency between droplets in an emulsion. The main aim of this review is to find information on the nonequilibrium behaviour of emulsions in shear flows due to coalescence and break-up of droplets. The results of this search provide possible experimental ways to investigate the coalescence rate in a Couette device, which is the goal of the work. These methods include :

1. Detection of the emitted light from the dye produced in the coalescence process;
2. Dynamic light scattering from emulsions;
3. Investigation of reological properties of nonstable concentrated emulsions using rheometrical devices.

From a theoretical point of view, the Smoluchowski theory with simple approximations for hydrodynamic interactions is considered as a starting point for subsequent work. The first, qualitative, experiments to find the probability of coalescence for a "water in oil" emulsion in a counter rotating the Couette device were carried out using a CDD camera. At low shear rates the unimodal distribution function for droplet diameters of the dispersed phase relaxes to a bimodal distribution function of stable emulsions. The tests were carried out for different values of the continuous phase viscosity (500 M, 750 M, 1000 M) and small volume fractions of the dispersed phase ($< 8\%$). An increase of the rupture time of the film between the colliding droplets and an increase of the time for relaxation of the emulsion to a steady state were observed when the viscosity of the continuous phase was increased.

For the following period, we plan to investigate the experimental conditions needed for item 1 (see above), to investigate the feasability of items 2, 3 and to continue the literature search.

Sub-Task 2.3. Industrial Experiments (URV, Total)

URV : Liquid/liquid stirred vessel test case

One of the industrial test cases in task 2.3 is the case of liquid/liquid dispersions in stirred vessels. Stirred vessels are challenging geomtries when it comes to two-phase modelling, as the degree of agitation is rather hetorogeneous throughout the vessel. As a result, various regimes of coalescence and break-up may be found. Although the individual droplets in the vessel may each experience very different local flow conditions, the mixing ensures a more or less uniform droplet size distribution throughout the vessel. Some experiments on concentrated W/O emulsions have already been published[2]. In these systems, the presence of emulsifier effectively prevents coalescence. It was found that the volume fraction does not significatly influence the break-up behaviour.

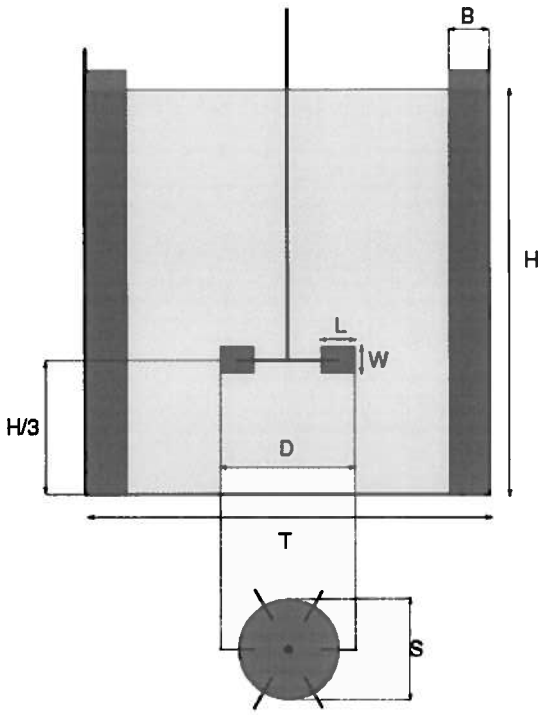

Figure 4: Geometry for liquid-liquid stirred vessel.

Some preliminary experiments were carried out on O/W emulsions. The emulsification is carried out in a stirred vessel, scaled to the Rushton standards, see figure 4:

$$\begin{aligned} H = T \quad & D = T/3 \\ S = T/4 \quad & L = T/12 \\ W = T/15 \quad & B = T/10 \end{aligned}$$

Samples are taken from the vessel, and immediately diluted in an aqueous solution of emulsifier. The droplet size distribution was measured using a Malvern Mastersizer static light scattering apparatus. The samples proved to be stable enough during handling. There is some concern that in systems without surfactant (where coalescence does play a significant role) can not be sufficiently stabilised to be measured on the Malvren Mastesizer, as some shear is generated in the dispersion to pump is through the measuring cell. In that case, the droplet size distribution should be analysed manually, from microscopy photographs.

Figure 5 shows the median droplet size as a function of the volume fraction of dispersed phase. Two extreme cases were investigated: 1. corn syrup solution (viscosity: $16mPa.s$) as a continuous phase, at a stirrer speed of 800 rpm, 2. pure water (viscosity: 1 mPa.s) as a continuous phase, at a stirrer speed of 400 rpm. The dispersed phase was a triglyceride oil (viscosity: $50mPa.s$) is both cases. As expected, we find the smallest droplets in case 1. As in the experiments [2], the droplet size does not depend on the volume fraction of dispersed phase.

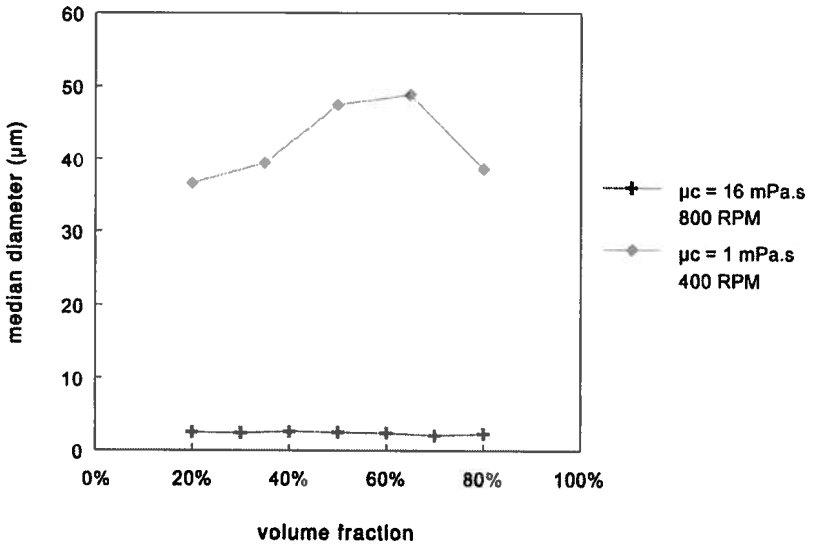

Figure 5: Median droplet size as a function of the volume fraction of dispersed phase in the stirred vessel

In case 2, however, we see, at low volume fractions, an increase of the droplet size with increasing volume fraction, suggesting that coalescence does play a role, and the droplet size is determined by a dynamic equilibrium between break-up and coalescence. Above a volume fraction of approx. $60 - 70\%$, the droplet size decreases with increasing volume fraction. This may be due to a viscosity effect: as a result of the increase in viscosity with increasing volume fraction dispersed phase, a transition from the inertial to the viscous break-up regime may occur, and the dynamic equilibrium between break-up and coalescence shifts considerably.

It is our intention to generate more data from this system, at intermediate points in the parameter space (variables: stirrer rpm and continuous phase viscosity). In addition, we want to perform experiments in systems lacking stabilization by surfactants, where coalescence plays a more significant role. It is expected that the droplet sizes will be much larger under those conditions. There is some concern that the droplet sizing equipment generates too much shear, causing break-up of the droplets during size analysis. In that case, we have to resort to manual analysis of microscopy photographs.

Sub-Task 3.1. Algorithm Development.

IC

The aim of this task is to evaluate the deficiencies of the algorithm developed in the previous BRITE project, and to investigate alternative strategies to find a more stable approach. One problem with the current formulation of the system is the force coupling between the phases, which causes numerical problems when trying to converge the sys-

tem. In addition, the mathematical structure of the equations is problematic, becoming ill-defined when the phase fraction tends to zero. Some theoretical work has been done to reformulate the equations to overcome these deficiencies and to devise numerical strategies robust enough to deal with the coupling. A project report on these issues is being prepared. In addition, a suite of test cases is being constructed, including input from the industrial partners, which any successful code will have to be able to calculate.

Computational Dynamics

Information from all users of the two-phase version of STAR (principally the partners in the previous project) about the behaviour of the code under various circumstances is being gathered and collated. This, together with experience with the code at CD, is valuable input to the algorithm development. The main problem with the algorithm developed in BRITE-II is that it is not robust in terms of convergence. As far as the numerics are concerned (i.e. neglecting issues of the formulation of the equations and their mathematical behaviour), the following problems have been observed in debugging various cases :

- Coupling of the continuity equations (currently explicit).
- Insensitivity of the mass residual to phase-specific information.
- Bounding of the phase fraction α.
- Symmetry of the algorithm under interchange of phases.
- Asymptotic limits of phase fraction at 0 and 1.

Investigation into some of these problems is continuing. This includes reformulation of the volume fraction equation to eliminate continuity problems, and modification of the pressure correction equation to take account of phase-specific information.

In addition to this work, suggestions have been made of test cases of physical importance or of industrial relevance, which will be of use in testing the limits of the code.

1.3 Effort Compared to Plan

Due to the delays in recruitment of staff at all the Universities, progress on some of the tasks has not been on target. In particular tasks 1.1 (?) and 2.2 (?) are somewhat behind schedule. However, although personnel have been appointed later than expected, work by permanent academic staff (project supervisors) at the Universities was put in and this means that some progress has nonetheless been make on all tasks, albeit not according to plan.

One possibility of recovering some of the lost time is through recruitment of additional temporary staff. However, it is too early to determine whether this contingency plan will be needed, and a decision on it should be made later towards the end of year 1.

1.4 Planned Activities for Forthcoming Period

2 Management and Coordination Aspects

Two meeting were held during the six month period. The first was held in January 1998 at Imperial College in London to launch the project on the technical front. The purpose of

the meeting was to open the technical exchange and discussion between the partners all of whom were represented. Problems with recruitment at the Universities were highlighted and this was almost certain to have an impact on the planned work. Some partners suggested that the project start date should be delayed to allow time for recruitment but subsequent enquiries with the CEC established that such a postponement was not permitted. The partners were made aware of the possible disruption this delay would have on the work programme.

The second meeting was held in February 1998 at the CEC in Brussels in the presence of the Project Officer. This was the official launch meeting during which the Project Officer outlined the requirements of the CEC and explained some of the procedures that have to be followed. The problem with recruitment was brought to the attention of the Officer.

A progress meeting in Toulouse was arranged for July 1998.

The advance payment from the CEC made to the Coordinator was distributed to all partners proportionately to their overall budgets.

A draft Consortium Agreement was put together in a collaborative effort between URV and IC. The document has been put to the partners and is to be discussed at the next meeting in July.

2.1 Personnel

During the report period, a Research Associate (Dr. G. Tabor) and a Research Assistant (Mr. Henrik Rusche) have been appointed at IC to work on the project. This brings the IC team to its full complement.

At TU, two appointments have been made which would bring the team there to full strength. The personnel are: Dr..... and.....

At INPT of the two research assistants needed for the project, only one has been appointed at the Chemical Engineering department (Mr.....). It is anticipated that the other assistant will be appointed at the department of Fluid Mechanics in the autumn when the academic year ends and new graduates appear on the labour market.

All industrial partners have appointed a member of staff to the project.

References

[1] Ubbink, O.: *Numerical Prediction of Two Fluid Systems with Sharp Interfaces*, PhD thesis, Imperial College, 1997.

[2] Groeneweg, F., van Dieren, F., and Agterof, W. G. M.: "Droplet break-up in a stirred water-in-oil emulsion in the presence of emulsifiers", *Colloids and Surfaces*, A91:207, 1994.

Outline of Henry's Algorithm

G.Tabor

January 11, 1999

1 Phase Fraction Equations.

The basic equations are

$$\begin{aligned}\frac{\partial \alpha\rho_a}{\partial t} + \nabla.(\alpha\rho_a \mathbf{U}_a) &= 0 \\ \frac{\partial \beta\rho_b}{\partial t} + \nabla.(\beta\rho_b \mathbf{U}_b) &= 0\end{aligned}$$

We can write

$$\overline{\rho}\widetilde{\mathbf{U}} = \alpha\rho_a \mathbf{U}_a + \beta\rho_b \mathbf{U}_b \tag{1}$$

where

$$\overline{\rho} = \alpha\rho_a + \beta\rho_b$$

$$\widetilde{\alpha} = \frac{\rho_a \alpha}{\overline{\rho}} \quad , \quad \widetilde{\beta} = \frac{\rho_b \beta}{\overline{\rho}}$$

Thus

$$\widetilde{\mathbf{U}} = \mathbf{U}_a - \widetilde{\beta}\mathbf{U}_r$$

Now dividing the continuity eq. through by ρ_a

$$\begin{aligned}\frac{\partial \alpha}{\partial t} + \nabla.(\alpha \mathbf{U}_a) &= \frac{\partial \alpha}{\partial t} + \nabla.(\alpha\widetilde{\mathbf{U}}) + \nabla.(\alpha\widetilde{\beta}\mathbf{U}_r) \\ &= \frac{\partial \widetilde{\alpha}}{\partial t} + \nabla.(\widetilde{\alpha}\widetilde{\mathbf{U}}) + \nabla.(\widetilde{\alpha}\widetilde{\beta}\mathbf{U}_r) \\ &= 0\end{aligned}$$

where the last step follows from multiplying through by $\rho_a/\overline{\rho}$.

In the code the α equation takes the form

$$\frac{\partial \alpha}{\partial t} + \nabla.(\phi\alpha) + \nabla.(\beta\phi_r\alpha) = \nabla.[C_\alpha \nu_t \nabla\alpha] \tag{2}$$

where the fluxes are

$$\phi = \alpha_F \phi_a + \beta_F \phi_b \quad (3)$$
$$\phi_r = \phi_a - \phi_b \quad (4)$$

and $_F$ refers to values of the variable evaluated on the cell face.

2 Momentum Equations

To conditional average an expression we multiply by an indicator function $\mathcal{I}$ and then ensemble average. The following commutation rules apply

$$\overline{\mathcal{I}\nabla \circ Q} = \nabla \circ (\alpha \overline{Q}) - \widehat{\overline{Q \circ \mathbf{n}_\alpha}\Sigma}$$
$$\overline{\mathcal{I}\frac{\partial Q}{\partial t}} = \frac{\partial \alpha \overline{Q}}{\partial t} - \widehat{\overline{Q\mathbf{U}_S.\mathbf{n}_\alpha}\Sigma}$$

where $\circ$ represents some sort of tensor product.

The NS equation is

$$\frac{\partial \rho \mathbf{U}}{\partial t} + \nabla.\rho \mathbf{U} \otimes \mathbf{U} = -\nabla p + \nabla.\sigma + \rho \mathbf{g} \quad (5)$$

where

$$\sigma = \mu \left(\nabla \mathbf{U} + \nabla \mathbf{U}^T - \frac{2}{3}\mathbf{I}\nabla.\mathbf{U} \right) \quad (6)$$

Multiplying through by $\mathcal{I}$ and averaging gives

$$\frac{\partial \alpha \overline{\rho_a \mathbf{U}_a}}{\partial t} - \widehat{\overline{\rho_a \mathbf{U}_a (\mathbf{U}_S.\mathbf{n}_a)}\Sigma} + \nabla.\alpha \overline{\rho_a \mathbf{U}_a \otimes \mathbf{U}_a} - \widehat{\overline{\rho_a \mathbf{U}_a \otimes \mathbf{U}_a.\mathbf{n}_a}\Sigma}$$
$$= -\nabla \alpha \overline{p}_a + \widehat{\overline{p\mathbf{n}_a}\Sigma} + \nabla.\alpha \sigma_a - \widehat{\overline{\sigma_a.\mathbf{n}_a}\Sigma} \quad (7)$$

We have implicitly used the Boussinesq hypothesis here : the ensemble averaging will produce a Reynolds stress term, which we have modelled as a correction to the viscosity in σ_a. We can write

$$\overline{\rho \mathbf{U}} = \overline{\rho} \widetilde{\mathbf{U}} \quad (8)$$

and

$$\overline{\rho \mathbf{U} \otimes \mathbf{U}} = \overline{\rho} \widetilde{\mathbf{U} \otimes \mathbf{U}} = \overline{\rho} \widetilde{\mathbf{U}} \otimes \widetilde{\mathbf{U}} + \overline{\rho} \widetilde{\mathbf{U}'' \otimes \mathbf{U}''}$$
$$\approx \overline{\rho} \widetilde{\mathbf{U}} \otimes \widetilde{\mathbf{U}} \quad (9)$$

The surface pressure term becomes

$$\widehat{\overline{p\mathbf{n}_a}\Sigma} \approx \overline{p}_I \frac{\mathbf{n}_a}{\Xi}\Sigma = \overline{p}_I \nabla \alpha \quad (10)$$

with $\overline{p}_I$ the interface pressure term.

Substituting these expressions in equation (7) gives

$$\begin{aligned}\frac{\partial \alpha \overline{\rho}_a \widetilde{\mathbf{U}}_a}{\partial t} + \nabla . \left[\alpha \overline{\rho}_a \widetilde{\mathbf{U}_a} \otimes \widetilde{\mathbf{U}_a}\right] &= -\nabla \alpha \overline{p}_a + \overline{p}_I \nabla \alpha \\ &\quad + \nabla . \alpha \sigma_a + \overline{\rho}_a \alpha \mathbf{g} + \mathbf{M} \end{aligned} \tag{11}$$

where $\mathbf{M}$ contains all the surface terms, which will be modelled in terms of various interfacial force terms. If we assume $\overline{p}_a = \overline{p}_I = \overline{p}_b = \overline{p}$, then the pressure term can be rewritten :

$$-\nabla \alpha \overline{p}_a + \overline{p}_I \nabla \alpha = -\alpha \nabla \overline{p} \tag{12}$$

Let us assume that both phases are incompressible, i.e. $\overline{\rho}_a =$ constant. We can divide through by the density

$$\frac{\partial \alpha \widetilde{\mathbf{U}}_a}{\partial t} + \nabla . \left[\alpha \widetilde{\mathbf{U}_a} \otimes \widetilde{\mathbf{U}_a}\right] = -\frac{1}{\overline{\rho}_a} \alpha \nabla \overline{p} + \nabla . \frac{\alpha \sigma_a}{\overline{\rho}_a} + \alpha \mathbf{g} + \frac{\mathbf{M}}{\overline{\rho}_a} \tag{13}$$

and similarly for the other phase

$$\frac{\partial \beta \widetilde{\mathbf{U}}_b}{\partial t} + \nabla . \left[\beta \widetilde{\mathbf{U}_b} \otimes \widetilde{\mathbf{U}_b}\right] = -\frac{1}{\overline{\rho}_b} \beta \nabla \overline{p} + \nabla . \frac{\beta \sigma_b}{\overline{\rho}_b} + \beta \mathbf{g} - \frac{\mathbf{M}}{\overline{\rho}_b} \tag{14}$$

We now look to eliminate α (and β) throughout the equation. Expanding the divergence term gives

$$\nabla . (\alpha \mathbf{U}_a \otimes \mathbf{U}_a) = \alpha \nabla . (\mathbf{U}_a \otimes \mathbf{U}_a) + \mathbf{U}_a \nabla . (\alpha \mathbf{U}_a) - \mathbf{U}_a \alpha \nabla . \mathbf{U}_a \tag{15}$$

Expanding the time derivative provides the term $\mathbf{U}_a \frac{\partial \alpha}{\partial t}$; using the phase fraction equation, we can now write the momentum equation as

$$\frac{\partial \mathbf{U}_a}{\partial t} + \nabla . [\mathbf{U}_a \otimes \mathbf{U}_a] - \mathbf{U}_a \nabla . \mathbf{U}_a = -\frac{\nabla \overline{p}}{\overline{\rho}_a} + \frac{1}{\alpha} \nabla . \frac{\alpha \sigma_a}{\overline{\rho}_a} + \mathbf{g} + \frac{\mathbf{M}}{\overline{\rho}_a \alpha} \tag{16}$$

and similarly for the phase b.

We now turn our attention to the stress term. We can expand

$$\begin{aligned}\frac{1}{\alpha} \nabla . \frac{\alpha \sigma_a}{\overline{\rho}_a} &= \nabla . \frac{\sigma_a}{\overline{\rho}_a} + \frac{\sigma_a}{\overline{\rho}_a} . \frac{\nabla \alpha}{\alpha} \\ &= \nabla . \left[\nu_{eff} \left(\nabla \mathbf{U}_a + \nabla \mathbf{U}_a^T - \frac{2}{3} \mathbf{I} \nabla . \mathbf{U}_a\right)\right] \\ &\quad + \nu_{eff} \left(\nabla \mathbf{U}_a + \nabla \mathbf{U}_a^T - \frac{2}{3} \mathbf{I} \nabla . \mathbf{U}_a\right) . \frac{\nabla \alpha}{\alpha} \\ &= \nabla . \left[\nu_{eff} \left(\nabla \mathbf{U}_a + \nabla \mathbf{U}_a^T - \frac{2}{3} \mathbf{I} \nabla . \mathbf{U}_a\right)\right] \\ &\quad + \left(\nu_{eff} \frac{\nabla \alpha}{\alpha}\right) . \left(\nabla \mathbf{U}_a + \nabla \mathbf{U}_a^T - \frac{2}{3} \mathbf{I} \nabla . \mathbf{U}_a\right)\end{aligned}$$

where the last step follows since the stress term is symmetric. We can subsume the terms of the form $\nabla \mathbf{U}_a$ in the divergence terms (i.e. make them part of the transport). Substituting the above for the stress we have

$$\begin{aligned}\frac{\partial \mathbf{U}_a}{\partial t} &+ \nabla.\left[\mathbf{U}_a \otimes \mathbf{U}_a\right] - \mathbf{U}_a \nabla.\mathbf{U}_a - \nabla.\left(\nu_{eff} \nabla \mathbf{U}_a\right) - \left(\nu_{eff} \frac{\nabla \alpha}{\alpha}\right).\nabla \mathbf{U}_a \\ &= -\frac{\nabla \overline{p}}{\overline{\rho}_a} + \nabla.\left[\nu_{eff}\left(\nabla \mathbf{U}_a^T - \frac{2}{3}\mathbf{I}\nabla.\mathbf{U}_a\right)\right] + \nu_{eff}\left(\nabla \mathbf{U}_a^T - \frac{2}{3}\mathbf{I}\nabla.\mathbf{U}_a\right)\frac{\nabla \alpha}{\alpha} + \mathbf{g} + \frac{\mathbf{M}}{\overline{\rho}_a \alpha}\end{aligned}$$

Now taking the terms

$$\begin{aligned}\nabla.\left[\mathbf{U}_a \otimes \mathbf{U}_a\right] &- \mathbf{U}_a \nabla.\mathbf{U}_a - \left(\nu_{eff} \frac{\nabla \alpha}{\alpha}\right).\nabla \mathbf{U}_a \\ &= \nabla.\left[\mathbf{U}_a \otimes \mathbf{U}_a\right] - \mathbf{U}_a \nabla.\mathbf{U}_a + \mathbf{U}_a \nabla.\left(\nu_{eff} \frac{\nabla \alpha}{\alpha}\right) \\ &\quad - \mathbf{U}_a \nabla.\left(\nu_{eff} \frac{\nabla \alpha}{\alpha}\right) - \left(\nu_{eff} \frac{\nabla \alpha}{\alpha}\right).\nabla \mathbf{U}_a \\ &= \nabla.\left[\mathbf{U}_a \otimes \mathbf{U}_a\right] - \mathbf{U}_a \nabla.\left[\mathbf{U}_a - \nu_{eff} \frac{\nabla \alpha}{\alpha}\right] \\ &\quad - \mathbf{U}_a \nabla.\left(\nu_{eff} \frac{\nabla \alpha}{\alpha}\right) - \left(\nu_{eff} \frac{\nabla \alpha}{\alpha}\right).\nabla \mathbf{U}_a \\ &= \nabla.\left[\mathbf{U}_a \otimes \mathbf{U}_a\right] - \mathbf{U}_a \nabla.\left[\mathbf{U}_a - \nu_{eff} \frac{\nabla \alpha}{\alpha}\right] - \nabla.\left[\nu_{eff} \frac{\nabla \alpha}{\alpha} \otimes \mathbf{U}_a\right] \\ &= \nabla.\left[\left(\mathbf{U}_a - \nu_{eff} \frac{\nabla \alpha}{\alpha}\right) \otimes \mathbf{U}_a\right] - \mathbf{U}_a \nabla.\left[\mathbf{U}_a - \nu_{eff} \frac{\nabla \alpha}{\alpha}\right]\end{aligned}$$

and thus

$$\begin{aligned}\frac{\partial \mathbf{U}_a}{\partial t} &+ \nabla.\left[\left(\mathbf{U}_a - \nu_{eff} \frac{\nabla \alpha}{\alpha}\right) \otimes \mathbf{U}_a\right] - \mathbf{U}_a \nabla.\left[\mathbf{U}_a - \nu_{eff} \frac{\nabla \alpha}{\alpha}\right] - \nabla.\left(\nu_{eff} \nabla \mathbf{U}_a\right) \\ &= -\frac{\nabla \overline{p}}{\overline{\rho}_a} + \nabla.\left[\nu_{eff}\left(\nabla \mathbf{U}_a^T - \frac{2}{3}\mathbf{I}\nabla.\mathbf{U}_a\right)\right] + \nu_{eff}\left(\nabla \mathbf{U}_a^T - \frac{2}{3}\mathbf{I}\nabla.\mathbf{U}_a\right)\frac{\nabla \alpha}{\alpha} + \mathbf{g} + \frac{\mathbf{M}}{\overline{\rho}_a \alpha}\end{aligned}$$

together with a similar equation for the second phase.

We can define velocity fluxes

$$\begin{aligned}\phi_{\mathbf{U}_a} &= \phi_a - \nu_{eff_a} \frac{\nabla \alpha}{\alpha} \\ \phi_{\mathbf{U}_b} &= \phi_b - \nu_{eff_b} \frac{\nabla \beta}{\beta}\end{aligned}$$

with ν_{eff_a} as the total (laminar plus turbulent) viscosity in phase a. Coefficients for the virtual mass, drag, lift terms are all as normal. We define additional terms

$$\begin{aligned}\mathcal{VM}_a &= 1 + \frac{C_{VM} \rho_b \beta}{\rho_a} \\ \mathcal{VM}_b &= 1 + \frac{C_{VM} \rho_a \alpha}{\rho_b}\end{aligned}$$

With these we can write the momentum equations as

$$\begin{aligned}\frac{\partial \mathbf{U}_a}{\partial t} &+ \nabla.(\phi_{\mathbf{U}_a}\mathbf{U}_a) - (\nabla.\phi_{\mathbf{U}_a})\mathbf{U}_a - \nabla.\nu_{eff_a}\nabla\mathbf{U}_a \\ &-\nabla.\left[\nu_{eff_a}(\nabla\mathbf{U}_a - \frac{2}{3}\mathbf{I}\nabla.\mathbf{U}_a)\right] - \nu_{eff_a}\left[\frac{\nabla\alpha}{\alpha}.\left(\nabla\mathbf{U}_a^t - \frac{2}{3}\mathbf{I}\nabla.\mathbf{U}_a\right)\right] \\ &= \frac{\mathbf{g}}{\mathcal{VM}_a} - \frac{\beta C_D}{\rho_a \mathcal{VM}_a}\mathbf{U}_a - \frac{\beta}{\rho_a \mathcal{VM}_a}\left(C_F - C_{VM}\rho_b\frac{D\mathbf{U}_b}{Dt}\right) \end{aligned} \quad (17)$$

Operators $\mathcal{A}_a$ and $\mathcal{H}_a$ are defined in the usual way on this equation, and similarly for the b equation :

$$\begin{aligned}\frac{\partial \mathbf{U}_b}{\partial t} &+ \nabla.(\phi_{\mathbf{U}_b}\mathbf{U}_b) - (\nabla.\phi_{\mathbf{U}_b})\mathbf{U}_b - \nabla.\nu_{eff_b}\nabla\mathbf{U}_b \\ &-\nabla.\left[\nu_{eff_b}(\nabla\mathbf{U}_b - \frac{2}{3}\mathbf{I}\nabla.\mathbf{U}_b)\right] - \nu_{eff_b}\left[\frac{\nabla\beta}{\beta}.\left(\nabla\mathbf{U}_b^t - \frac{2}{3}\mathbf{I}\nabla.\mathbf{U}_b\right)\right] \\ &= \frac{\mathbf{g}}{\mathcal{VM}_b} - \frac{\alpha C_D}{\rho_b \mathcal{VM}_b}\mathbf{U}_b - \frac{\alpha}{\rho_b \mathcal{VM}_b}\left(C_F - C_{VM}\rho_a\frac{D\mathbf{U}_a}{Dt}\right) \end{aligned} \quad (18)$$

Here

$$\begin{aligned}\frac{D\mathbf{U}_a}{Dt} &= \frac{\partial \mathbf{U}_a}{\partial t} + \nabla.(\phi_a\mathbf{U}_a) - (\nabla.\phi_a)\mathbf{U}_a \\ \frac{D\mathbf{U}_b}{Dt} &= \frac{\partial \mathbf{U}_b}{\partial t} + \nabla.(\phi_b\mathbf{U}_b) - (\nabla.\phi_b)\mathbf{U}_b\end{aligned}$$

We make an initial estimate of the fluxes as

$$\begin{aligned}\phi_a^* &= \frac{\mathcal{H}_a.\delta A}{\mathcal{A}_a} + \frac{\beta C_D}{\rho_a \mathcal{VM}_a \mathcal{A}_a}\phi_b \\ \phi_b^* &= \frac{\mathcal{H}_b.\delta A}{\mathcal{A}_b} + \frac{\alpha C_D}{\rho_b \mathcal{VM}_b \mathcal{A}_b}\phi_a\end{aligned}$$

In terms of these quantities the pressure equation takes the form

$$\nabla.\left[\left(\frac{\alpha_F}{\rho_a \mathcal{A}_a \mathcal{VM}_a} + \frac{\beta_F}{\rho_b \mathcal{A}_b \mathcal{VM}_b}\right)\nabla p\right] = \nabla.(\alpha_F\phi_a^* + \beta_F\phi_b^*) \quad (19)$$

3 Pressure update algorithm.

The pressure update algorithm is complex.

1. An estimate of the individual phase fluxes is made in terms of their old values

$$\begin{aligned}\phi_a^* &= \frac{\mathcal{H}_a\delta A}{\mathcal{A}_a} + \frac{\beta C_D}{\rho_a \mathcal{VM}_a \mathcal{A}_a}\phi_b \\ \phi_b^* &= \frac{\mathcal{H}_b\delta A}{\mathcal{A}_b} + \frac{\alpha C_D}{\rho_b \mathcal{VM}_b \mathcal{A}_b}\phi_a\end{aligned}$$

(note the crossover of the flux terms).

2. The face-valued phase fractions α_F, β_F are evaluated from their cell-centred values.

3. Equation (19) is constructed and solved for p.

4. The individual phase fluxes are updated as

$$\begin{aligned} \phi_a &= \phi_a^* - \frac{1}{\rho_a \mathcal{A}_a \mathcal{V} \mathcal{M}_a} \|\delta A\| \nabla p \\ \phi_b &= \phi_b^* - \frac{1}{\rho_b \mathcal{A}_b \mathcal{V} \mathcal{M}_b} \|\delta A\| \nabla p \end{aligned}$$

5. Finally, the overall flux is evaluated using (3) :

$$\phi = \alpha_F \phi_a + \beta_F \phi_b$$

This will be referred to as *pressure update.*

4 Overall algorithm

We are now in a position to state the overall algorithm.

1. Solve the α-equation, eq. (2).

2. Calculate the physical coefficients C_D, C_{VM} etc.

3. Construct (but do not *solve*) the momentum equations (17), (18).

4. Execute the following loop $N = 4$ times :

   (a) Solve the α-equation

   (b) *Pressure update*

5. Evaluate the cell-centred velocities by integrating the appropriate fluxes over the cell. Evaluate the convective derivatives $D\mathbf{U}_a/Dt$, $D\mathbf{U}_b/Dt$.

6. Solve $k - \epsilon$ system of equations.